AD_____

Award Number: DAMD17-97-1-7105

TITLE: (alpha)2(beta)1 Integrin-Induced Breast Cancer Differentiation

PRINCIPAL INVESTIGATOR: Tetsuji Kamata, M.D., Ph.D.

CONTRACTING ORGANIZATION: The Scripps Research Institute
La Jolla, California 92037

REPORT DATE: August 2001

TYPE OF REPORT: Annual Summary

PREPARED FOR: U.S. Army Medical Research and Materiel Command
Fort Detrick, Maryland 21702-5012

REPORT DOCUMENTATION PAGE

Form Approved
OMB No. 074-0188

1. AGENCY USE ONLY (Leave blank)	2. REPORT DATE	3. REPORT TYPE AND DATES COVERED
	August 2001	Annual Summary (1 Aug 97 - 31 Jul 01)

4. TITLE AND SUBTITLE
(alpha)2(beta)1 Integrin-Induced Breast Cancer Differentiation

5. FUNDING NUMBERS
DAMD17-97-1-7105

6. AUTHOR(S)
Tetsuji Kamata, M.D., Ph.D.

7. PERFORMING ORGANIZATION NAME(S) AND ADDRESS(ES)
The Scripps Research Institute
La Jolla, California 92037

E-Mail: grants@scripps.edu

8. PERFORMING ORGANIZATION REPORT NUMBER

9. SPONSORING / MONITORING AGENCY NAME(S) AND ADDRESS(ES)
U.S. Army Medical Research and Materiel Command
Fort Detrick, Maryland 21702-5012

10. SPONSORING / MONITORING AGENCY REPORT NUMBER

11. SUPPLEMENTARY NOTES
Report contains color

12a. DISTRIBUTION / AVAILABILITY STATEMENT
Approved for Public Release; Distribution Unlimited

12b. DISTRIBUTION CODE

13. Abstract *(Maximum 200 Words)* *(abstract should contain no proprietary or confidential information)*
Cell adhesive events play essential roles in the pathophysiology of breast cancer. Two important biological phenomena have been shown to depend upon integrins. The differentiation of breast cancer cells depends upon the expression of α2β1 integrin on the cell surface. The creation of distant metastasis is supported by the association of breast cancer cells with platelets. This association depends on the interaction between the activated αVβ3 integrin on the breast cancer cell surface with the activated αIIbβ3 integrin on the platelet surface. Thus, it is reasonable to assume that modulation of the function of those integrins may lead to the differentiation of poorly-differentiated breast cancer or the prevention of distant metastasis to other organs. To attain this goal, it is imperative to understand the precise mechanisms of integrin-ligand interaction. In this project I identified the ligand contact surfaces of α2β1 and αIIbβ3 integrins. The ligand contact site in α2β1 is composed of several discontinuous amino acid residues surrounding the MIDAS in the α2 I domain. The αIIbβ3 ligand binding interface is located on the outer edge and side of the propeller centering on β-sheet 3 of the αIIb β-propeller domain. These findings may form the basis for developing therapeutics for breast cancer.

14. SUBJECT TERMS
Breast Cancer, Integrin, Collagen, Laminin

15. NUMBER OF PAGES
28

16. PRICE CODE

17. SECURITY CLASSIFICATION OF REPORT	18. SECURITY CLASSIFICATION OF THIS PAGE	19. SECURITY CLASSIFICATION OF ABSTRACT	20. LIMITATION OF ABSTRACT
Unclassified	Unclassified	Unclassified	Unlimited

Table of Contents

4. INTRODUCTION

Cell adhesive events play essential roles in many important physiological and pathological aspects in breast cancer, such as its differentiation (1, 2, 3) and metastatic properties. Loss of $\alpha 2\beta 1$ integrin expression is associated with the aggressive phenotype of breast cancer in patients (4). Artificial manipulation of $\alpha 2\beta 1$ integrin expression in breast cancer cell lines leads to the change in phenotype (5, 6).

These lines of evidence suggest that $\alpha 2\beta 1$ integrin-ligand interaction is crucial for breast cancer differentiation. These results suggest that modulation of integrin, particularly $\alpha 2\beta 1$, could be an important therapeutic target for breast cancer. Integrins also play critical roles in the pathogenesis of distant metastasis through interaction with vascular endothelial cells and their extracellular matrices. In general, the prerequisite step in creating hematogenous metastasis is for the tumor cells to withstand the shear force in the blood stream and arrest in the blood vessels. It has been shown that platelet thrombus provides melanoma cells stable anchorage that withstand the shear force. This stable interaction between platelets and melanoma cells was dependent on $\alpha IIb\beta 3$ on platelets and $\alpha V\beta 3$ on melanoma cells (7). In breast cancer, the $\alpha V\beta 3$ integrin characterizes the metastatic phenotype, since it is up-regulated in invasive tumors and distant metastases. However, it is not yet known why this integrin is associated with the metastatic phenotype. Recently, Felding-Habermann *et al.* have shown that breast cancer cell arrest during blood flow is supported by activated $\alpha V\beta 3$ through its interaction with platelets (8). Thus, it is reasonable to assume that breast cancer cells metastasize to distant organs utilizing platelets as anchorage. It is therefore important to characterize the interaction between tumor cells and platelets. Previous reports suggest that $\alpha IIb\beta 3$ on platelets, other unknown molecules on the tumor cell side, and bridging adhesive proteins are involved in this interaction (7, 9). Therefore the $\alpha IIb\beta 3$-adhesive protein interaction could be a key target for creating the therapeutic modalities to prevent hematogenous metastasis. The purpose of this study is to elucidate the binding mechanisms of pathophysiologically relevant integrins in breast cancer, namely $\alpha 2\beta 1$ and $\beta 3$ integrins.

5. BODY

5.a. Collagen contact site in α2β1

5.a.1. Discontinuous multiple amino acid residues in the I domain are required for collagen binding

The MIDAS (metal ion-dependent adhesion site) face, the putative ligand binding face, of the α2 I domain is composed of four discontinuous loop structures. The βA-α1, α3-α4, and βD-α5 loops contain amino acid residues that compose the MIDAS motif, which is critical for divalent cation coordination (10, 11). These amino acid residues are relatively well conserved among different I domains. On the contrary, the amino acid sequences of the βE-α6 loop are variable. Notably, there are five amino acid insertions within this loop in collagen-binding α1, α2, α10, and α11 integrin I domains. The crystal structure of α2 I domain revealed that these inserted residues constitute an extra C-helix within the βE-α6 loop (12). This C-helix creates a groove on top of the MIDAS face in which a collagen triple helix is predicted to dock. Therefore the C-helix was predicted to be the major determinant of collagen binding. Based on the crystal structure of α2 I domain, I replaced loops surrounding the MIDAS motif with the homologous loops of αL and examined the effect on ligand binding (see the 1999 annual report and manuscript 1 for details). The L βA-α1 and L α3-α4 mutants almost completely abolished collagen adhesion even though the MIDAS motif is maintained. The L βD-α5 mutant partially affected collagen adhesion. On the other hand, the del αC mutant, which is missing most of the βE-α6 loop including the C-helix, did not have any impact on collagen adhesion even though αC is predicted to have a collagen contact site (12). These results suggest that the collagen contact sites are localized in the βA-α1, α3-α4, and βD-α5 loops of the α2 I domain, and that the C-helix does not contain any energetically important collagen contact sites. To further characterize the collagen-contact face, I introduced multiple point mutations into the residues within those critical loops. Consistent with the results from loop-swapping mutagenesis, I found that Ser-153, Ile-156, and Tyr-157 in βA-α1; Gln-215 and Gly-218 in α3-α4; and Gly-255 in βD-α5, in addition to the previously reported Asp-151, Thr-221 and Asp-254, are critical for collagen binding. In addition, mutation of Asn-154, Ser-155, Asp-219 and His-258 had a mild blocking effect on collagen binding when collagen type I was immobilized at 2 μg/ml. Consistent with the data obtained from the del αC mutant, mutations in the amino acid residues in the βE-α6 loop did not affect collagen binding at all (see manuscript 1 for detail). These results suggest that the energetically important collagen contact sites are localized in relatively conserved sequences surrounding the MIDAS motif.

5.a.2. α2 I domain/collagen binding model

In collaboration with Dr. Liddington, we created an α2 I domain/collagen docking model based on the mutagenesis data. In the crystal structure, Asp-151, Ser-153, Ser-155, Thr-221 and Asp-254 are involved in the coordination of the cation. Ile-156 is totally buried in the molecule. Mutations of Gln-215, Gly-218 and Gly-255 are either buried or likely to disrupt the MIDAS motif. In contrast, Asn-154, Tyr-156, Asp-219, and His-258 are totally exposed on the surface of the molecule, suggesting that these residues make direct contact with collagen. Recently, a short synthetic triple-helical peptide, representing residues 502-516 of the collagen type I α_ chain, has been shown to support purified α_β_ and recombinant α_ I-domain binding (13). The Glu and Arg residues in the GER triplet were found to be essential for recognition by the α_ I-

domain. In the current model, Asn-154, Tyr-157, Asp-219, and His-258 make direct contact with collagen, and the arginine from the GER motif makes a salt bridge to Glu-256 (see manuscript 1 for detail). In addition, Tyr-285 from the C-helix also makes direct contact with collagen. However, current mutagenesis data suggests that this is not energetically important.

The actual crystal structure of a complex between the α2 I domain and a collagen triple helical peptide has been published. The crystal structure has a striking similarity to the docking model we created, except that the αC helix undergoes extensive conformational change and moves away from the collagen triple helix (14). This result completely agrees with our mutagenesis data since we could not find any critical residues for collagen binding in the αC helix, contrary to the original assumption that the αC helix contains a critical collagen binding site (12). All the amino acid residues essential for collagen binding in our study make direct contact with collagen in the crystal structure. These results indicate that we can accurately predict the ligand binding sites in integrins using mutagenesis data.

5.b. Ligand binding interface of αIIb

5.b.1. Swapping mutagenesis of αIIb

Previous studies on breast cancer and other cancer cells suggest that cancer cells use αVβ3 or unknown receptors on their surface to bind to αIIbβ3 on platelets via bridging molecules for anchorage (7, 8, 9). So far, it is not clear what adhesive proteins bridge between the tumor cells and activated platelets under flow conditions. However, several reports suggest that tumor cells may utilize fibrinogen or vWF (vonWillebrand factor) at least in part as a bridging molecule (7, 9, 15). The αIIbβ3 integrin is a prototypic integrin that is also known as Glycoprotein IIb-IIIa (GPIIb-IIIa). The ligand binding specificity of αIIbβ3 is rather promiscuous and it also binds to proteins such as fibronectin, vitronectin, and thrombospondin in an RGD-dependent manner, as well as fibrinogen and vWF (16). Since αIIbβ3 is the common molecule utilized for anchorage by a variety of cancer cells, we sought to determine the ligand binding site in αIIbβ3.

To localize the ligand binding site in αIIbβ3, I used the same strategy for localizing the collagen contact site in α2β1. The first step is to create a swapping mutant of αIIb in which a particular amino acid sequence is replaced by the homologous sequence from a different integrin alpha subunit that has different ligand binding specificity. Since the three-dimensional structure of integrin alpha subunit is not yet known, except for the I domain of the I domain-containing integrins, it is difficult to determine what surface-exposed segment can be swapped without affecting the gross conformation or surface expression. I first aligned the amino acid sequences of αIIb with α4 and α5, which do not bind to fibrinogen or vWF. Based on the secondary structure prediction of α4, predicted loops between the β-strands were chosen for swapping mutagenesis (see the 2000 annual report for details).

5.b.2. Eight discontinuous predicted loops in αIIb are essential for fibrinogen binding to αIIbβ3 integrin.

Fibrinogen binding to cells expressing mutant αIIbβ3 were examined as previously described (17, 18). Out of 27 swapping mutants we created, W2A, W2C, W3A, W3C, W3D, W4A, W4C, and W5A mutants did not bind fibrinogen, even though they all bound to the activating mAb PT25-2 and showed comparable αIIbβ3 expression levels. The W5D mutant did not bind to fibrinogen either in this system. However, it failed to bind to PT25-2. The W5D mutant had an intact

fibrinogen binding site, since it bound to fibrinogen using other activation methods (see the 2000 annual report for details). The binding of the ligand-mimetic antibody PAC-1 to those mutants was also examined. Similar to the fibrinogen binding results, W2A, W2C, W3A, W3C, W3D, W4A, and W5A mutants showed significantly reduced binding to PAC-1 upon activation with PT25-2. On the contrary, the W4C mutant, which showed impaired binding to fibrinogen, exhibited PAC-1 binding comparable to wt (Fig. 1).

5.b.3. Multiple discontinuous amino acid residues are essential for fibrinogen binding.

To minimize the effect on the overall conformation of αIIbβ3, point mutations were introduced into the regions that affect fibrinogen binding when swapped. We introduced alanine mutations into individual amino acid residues within the critical W2A, W2C, W3A, W3C, W3D, W4A, W4C, and W5A regions. Fig. 2 shows the fibrinogen binding to CHO cells expressing those mutants. The Ala mutation of Asp-74, Leu-84, and Phe-87 in W2A; Trp-110, His-112, and Trp-113 in W2C; Arg-147, Tyr-155, Phe-160, Asp-163, and Arg-165 in W3A; Tyr-189, Tyr-190, Phe-191, and Gly-193 in W3C; Ile-203, Phe-204, and Tyr-207 in W3D; Ser-222, Asp-224, Phe-231, and Asp-232 in W4A; Leu-264 in W4C; and Gln-284 and Met-285 in W5A almost completely blocked fibrinogen binding when replaced by alanine. The other mutations did not significantly affect fibrinogen binding. These point mutations affected mAb binding to various degrees (data not shown). These results indicate that specific residues essential for fibrinogen binding can be localized within the regions identified by swapping mutagenesis. Some of those residues most likely compose the fibrinogen contact site.

5.b.4. Molecular modeling of αIIb

In collaboration with Dr. Springer, we generated an αIIb β-propeller model based on the alignment of αIIb with the β-propeller domain of the beta subunit of heterotrimeric G protein (Fig. 3). The loops of each β-sheet or W are named after the β-sheets they connect. The 4-1 and 2-3 loops correspond to positions A and C, respectively, and are located very close to each other in the upper face of the model. The 1-2 and 3-4 loops correspond to positions B and D, respectively, and are located in the lower face of the model. Loop swaps that did or did not eliminate binding are shown as red and green, respectively, and individual alanine substitutions are similarly color coded and shown as spheres. The model reveals that the amino acid residues critical for ligand binding that were identified in this study are clustered in the outer edge of β-sheet 2-5. It is interesting that among these residues, Ile-203, Phe-204, and Tyr-207 in the 3-4 loop of W3 are located on the side of the β-propeller. The model predicts that the outer β4 strand between the critical 3-4 loop of W3 and the 4-1 loop of W4 is surface-exposed (shown as magenta in Fig. 3), and thus may constitute part of the ligand-binding interface. Consistent with this prediction, swapping mutation of the entire β4 strand (β4W3), and Ala mutation of Leu-212 and Leu-213 within the strand, disrupted ligand binding (Fig.4). The outer β4 strand between the 3-4 loop of W5 and the 4-1 loop of W6, which is not essential for ligand binding, is also surface-exposed in the model. In contrast, swapping mutation of the strand did not block ligand binding at all (data not shown). These results suggest that the ligand-binding interface may lie not only on the top face, but also on the side of the β-propeller toroid, centering on β-sheet 3. In fact, the sides contribute to ligand binding in many β-propellers (19, 20, 21). These side residues are clustered near those in the top of the β-propeller, and all may contribute to a common ligand-binding surface. Alternatively, they may have an indirect effect on the β-propeller or on a

neighboring domain.

Consistent with the proposed critical function of these residues in ligand binding, most of these surface-exposed residues are well conserved among human (22), rat (23), and mouse αIIb (18, 24), except that Leu-84 is replaced with Phe in rat and mose αIIb, Phe-205 is replaced with Ile in mouse and rat αIIb, and Tyr-190 and Ser-222 are replaced with homologous Phe and Thr, respectively, in mouse and rat sequences.

6. KEY RESEARCH ACCOMPLISHMENTS

a. Identification of the collagen contact site in the I domain of α2β1 integrin.
b. Generation of a collagen/α2 I domain docking model.
c. Mapping of a monoclonal antibody epitope in αIIb
d. Identification of the fibrinogen binding interface in αIIbβ3 integrin.
e. Generation of the β-propeller model of the αIIb subuit.

7. REPORTABLE OUTCOMES

7.a. Manuscripts

1. Kamata T, Liddington RC, Takada Y. Interaction between collagen and the alpha(2) I-domain of integrin alpha(2)beta(1): Critical role of conserved residues in the metal ion-dependent adhesion site (MIDAS) region. J Biol Chem 274:32108-11, 1999.
2. Puzon-McLaughlin W, Kamata T, Takada Y. Multiple discontinuous ligand-mimetic antibody binding sites define a ligand binding pocket in integrin alpha(IIb)beta(3). J Biol Chem 275:7795-802, 2000.

7.b. Presentations

Kamata T, Liddington RC, Takada Y. Identification of collagen contact site in alpha(2)beta(1) integrin: Critical role of conserved residues in the metal-dependent adhesion site (MIDAS) region. Department of Defense Breast Cancer Research Program Era of Hope Meeting 2000.

7.c. Development of cell lines

Numerous stable CHO cell lines expressing mutant alpha(2) integrin were established.

8. CONCLUSIONS

The collagen contact site in α2β1 integrin is composed of the amino acid residues Asn-154, Tyr-157, Asp-219, and His-258, which surround the MIDAS motif of the α2 I domain. These residues make direct contact with the collagen triple-helical peptide in the collagen/α2 I domain complex crystal structure.

Nine discontinuous short segments in αIIb are essential for αIIbβ3 binding to fibrinogen. Among the amino acid residues within those segments, Asp-74, Leu-84, Phe-87, Trp-110, His-112, Trp-113, Arg-147, Tyr-155, Phe-160, Asp-163, Arg-165, Tyr-189, Tyr-190, Phe-191, Gly-

193, Ile-203, Phe-204, Tyr-207, Leu-212, Leu-213, Ser-222, Asp-224, Phe-231, Asp-232, Leu-264, Gln-284, and Met-285 eliminated fibrinogen binding when mutated. These residues are clustered on the outer edge and side of the propeller centering on β-sheet 3 in the β-propeller model.

9. REFERENCES

1. C. H. Streuli, N. Bailey, M. J. Bissel, *J. Cell Biol.* **115**, 1383-1395 (1991).
2. V. M. Weaver, A. H. Fischer, O. W. Peterson, M. J. Bissell, *Biochem Cell Biol* **74**, 833-51 (1996).
3. C. H. Streuli, G. M. Edwards, *J Mammary Gland Biol Neoplasia* **3**, 151-63 (1998).
4. M. M. Zutter, H. R. Krigman, S. A. Santoro, *Am J Pathol* **142**, 1439-48 (1993).
5. P. J. Keely, A. M. Fong, M. M. Zutter, S. A. Santoro, *J Cell Sci* **108**, 595-607 (1995).
6. M. M. Zutter, S. A. Santoro, W. D. Staatz, Y. L. Tsung, *Proc Natl Acad Sci U S A* **92**, 7411-5 (1995).
7. B. Felding-Habermann, R. Habermann, E. Saldivar, Z. M. Ruggeri, *J Biol Chem* **271**, 5892-900 (1996).
8. B. Felding-Habermann, et al., *Proc Natl Acad Sci U S A* **98**, 1853-8 (2001).
9. O. J. McCarty, S. A. Mousa, P. F. Bray, K. Konstantopoulos, *Blood* **96**, 1789-97 (2000).
10. T. Kamata, Y. Takada, *J Biol Chem* **269**, 26006-10 (1994).
11. T. Kamata, W. Puzon, Y. Takada, *J Biol Chem* **269**, 9659-63 (1994).
12. J. Emsley, S. L. King, J. M. Bergelson, R. C. Liddington, *J Biol Chem* **272**, 28512-7 (1997).
13. C. G. Knight, et al., *J Biol Chem* **273**, 33287-94 (1998).
14. J. Emsley, C. G. Knight, R. W. Farndale, M. J. Barnes, R. C. Liddington, *Cell* **101**, 47-56 (2000).
15. S. Karpatkin, E. Pearlstein, C. Ambrogio, B. S. Coller, *J Clin Invest* **81**, 1012-9 (1988).
16. R. Pytela, M. D. Pierschbacher, M. H. Ginsberg, E. F. Plow, E. Ruoslahti, *Science* **231**, 1559-1562 (1986).
17. T. Kamata, A. Irie, M. Tokuhira, Y. Takada, *J Biol Chem* **271**, 18610-5 (1996).
18. W. Puzon-McLaughlin, T. Kamata, Y. Takada, *J Biol Chem* **275**, 7795-802 (2000).
19. V. Fulop, D. T. Jones, *Curr Opin Struct Biol* **9**, 715-21. (1999).
20. M. P. Panchenko, et al., *J Biol Chem* **273**, 28298-304. (1998).
21. E. ter Haar, S. C. Harrison, T. Kirchhausen, *Proc Natl Acad Sci U S A* **97**, 1096-100. (2000).
22. M. Poncz, et al., *J Biol Chem* **262**, 8476-82 (1987).
23. M. Poncz, P. J. Newman, *Blood* **75**, 1282-9 (1990).
24. M. A. Thornton, M. Poncz, *Blood* **94**, 3947-50. (1999).

10. APPENDICES

10.a. Bibliography of all publications and meeting abstracts

1. Kamata T, Liddington RC, Takada Y. Interaction between collagen and the alpha(2) I-domain of integrin alpha(2)beta(1): Critical role of conserved residues in the metal ion-dependent adhesion site (MIDAS) region. J Biol Chem 274:32108-11, 1999.

2. Puzon-McLaughlin W, Kamata T, Takada Y. Multiple discontinuous ligand-mimetic antibody binding sites define a ligand binding pocket in integrin alpha(IIb)beta(3). J Biol Chem 275:7795-802, 2000.

3. Kamata T, Liddington RC, Takada Y. Identification of collagen contact site in alpha(2)beta(1) integrin: Critical role of conserved residues in the metal ion-dependent adhesion site (MIDAS) region. Department of Defense Breast Cancer Research Program Era of Hope Meeting 2000.

10.b. List of personnel receiving pay from the research effort

Tetsuji Kamata

10.c. Figures 1 to 4

10.d. Journal Articles

1. Kamata T, Liddington RC, Takada Y. Interaction between collagen and the alpha(2) I-domain of integrin alpha(2)beta(1): Critical role of conserved residues in the metal ion-dependent adhesion site (MIDAS) region. J Biol Chem 274:32108-11, 1999.

2. Puzon-McLaughlin W, Kamata T, Takada Y. Multiple discontinuous ligand-mimetic antibody binding sites define a ligand binding pocket in integrin alpha(IIb)beta(3). J Biol Chem 275:7795-802, 2000.

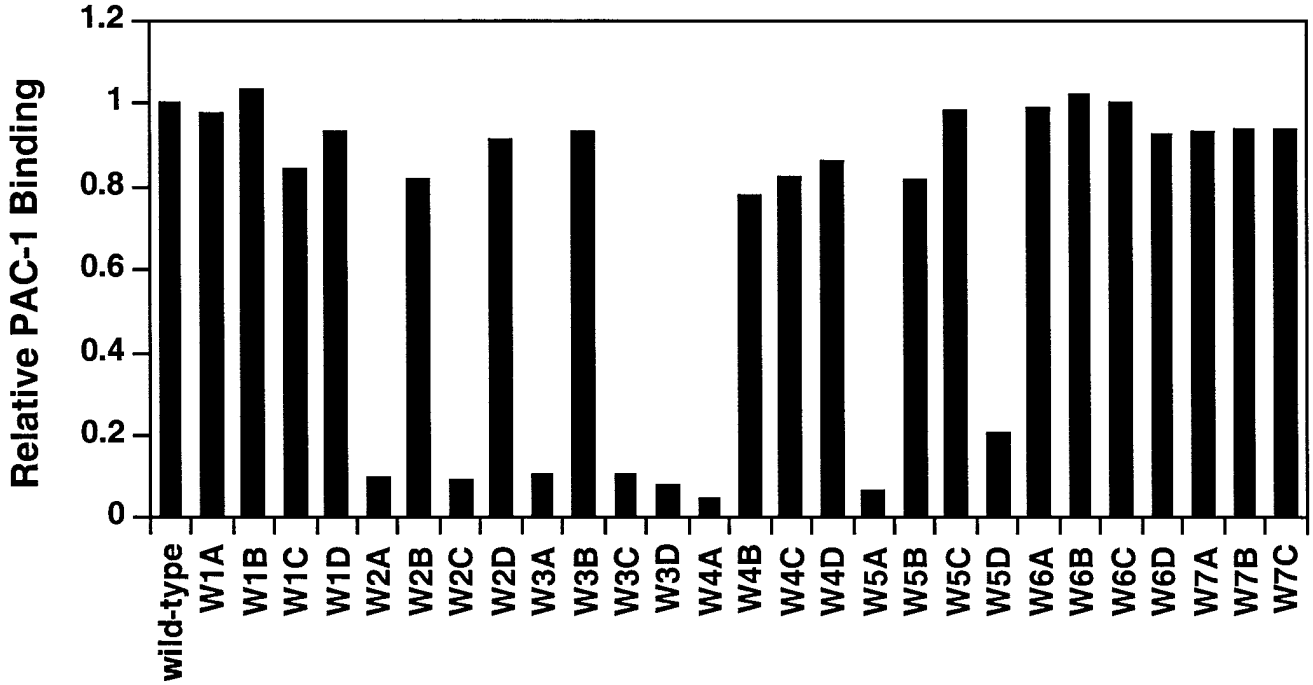

Fig. 1. PAC-1 binding to swapping mutants. β3-CHO cells transiently expressing αIIb mutants were stained either with PAC-1 in the presence of PT25-2 or with PL98DF6. Bound IgM (PAC-1) and IgG (PL98DF6) was detected with FITC-conjugated anti-mouse IgM or anti-mouse IgG, respectively. Percent PAC-1 binding was first normalized with αIIbβ3 expression with PL98DF6 (anti-αIIb). The normalized PAC-1 binding was divided by the normalized PAC-1 binding to cells expressing wt αIIbβ3 to obtain relative PAC-1 binding.

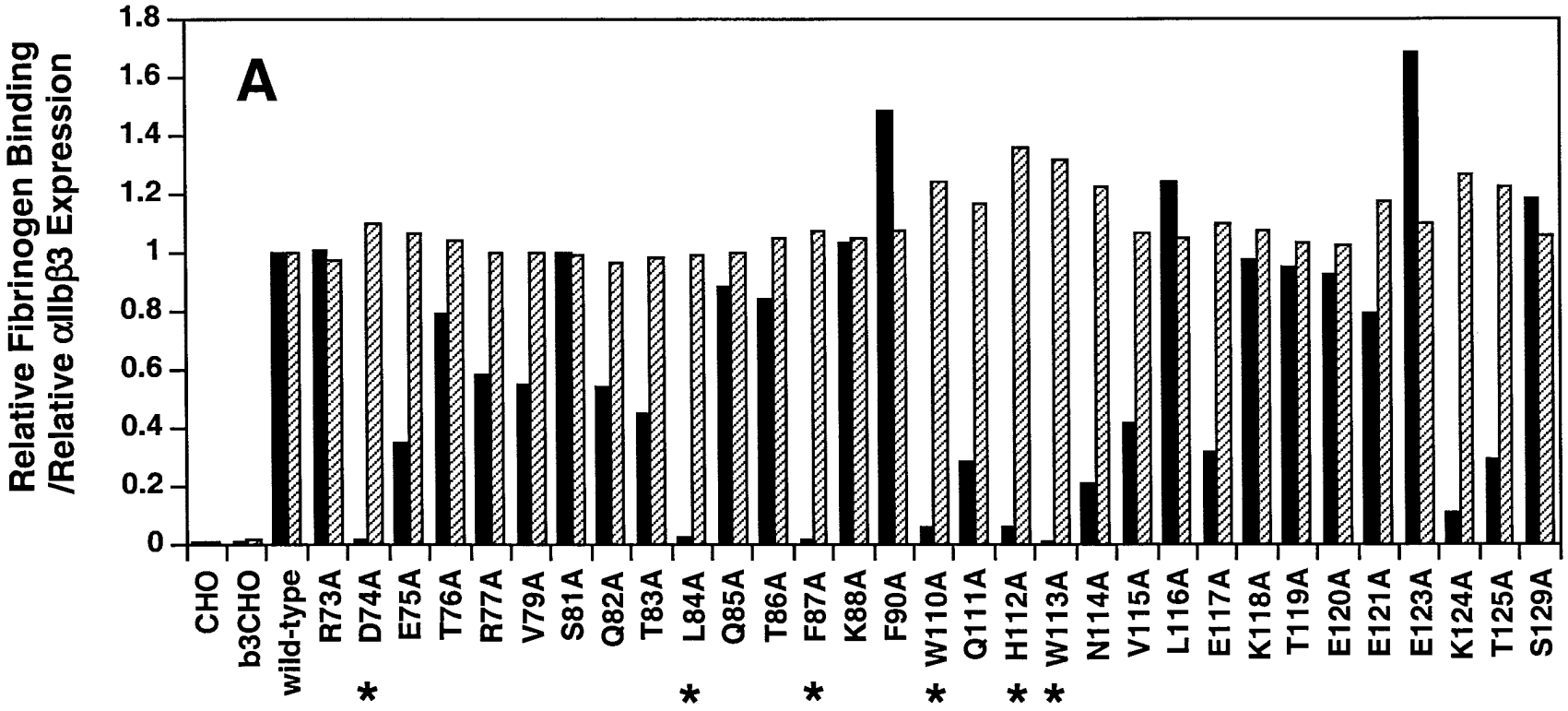

Fig. 2. Fibrinogen binding to αIIb point mutants. Individual amino acid residues within the predicted β-sheet 2 (A), β-sheet 3 (B), β-sheet 4 and 5(C) were mutated to Ala by site-directed mutagenesis. Mutant αIIb cDNAs were transiently expressed in β3-CHO. Cells were first stained with PL98DF6 followed by PE-conjugated anti-mouse IgG. After washing, cells were incubated with FITC-labeled fibrinogen in the presence of PT25-2 or normal mouse IgG. Fibrinogen binding to a gated subset of cells expressing αIIbβ3 at a high level (PE-positive) was analyzed in flow cytometry. Relative fibrinogen binding (solid bar) and relative αIIbβ3 expression (hatchet bar) were calculated as described in previous report. Fibrinogen binding to parent CHO and β3-CHO are included as controls. Mutants that exhibit fibrinogen binding less than 5 % of wild-type fibrinogen binding are marked with asterisks.

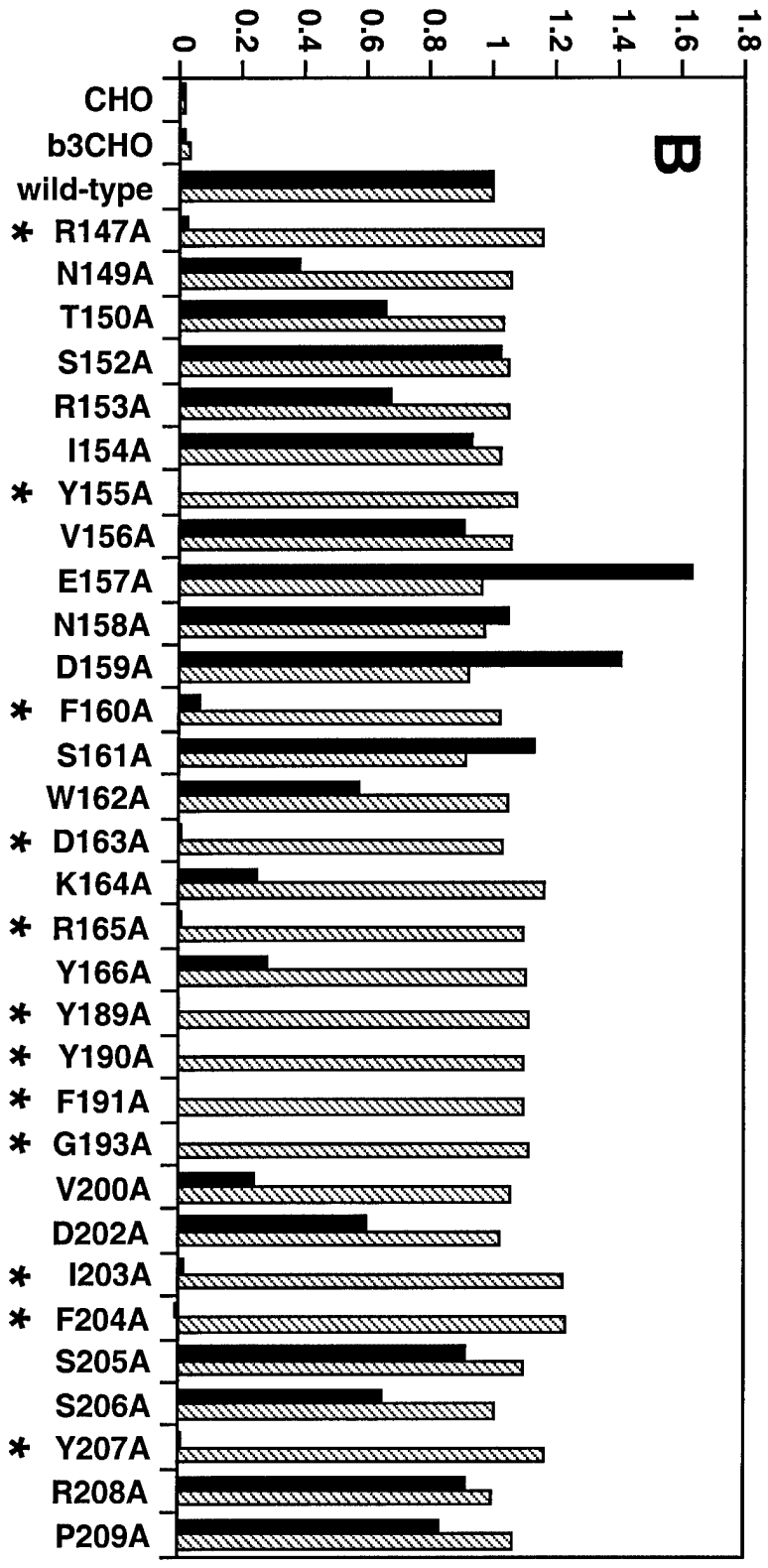
Relative Fibrinogen Binding
/Relative αIIbβ3 Expression
0
0.2
0.4
0.6
0.8
1
1.2
1.4
1.6
1.8
B
CHO
b3CHO
wild-type
* R147A
N149A
T150A
S152A
R153A
I154A
* Y155A
V156A
E157A
N158A
D159A
* F160A
S161A
W162A
* D163A
K164A
* R165A
Y166A
* Y189A
* Y190A
* F191A
* G193A
V200A
D202A
* I203A
* F204A
S205A
S206A
* Y207A
R208A
P209A

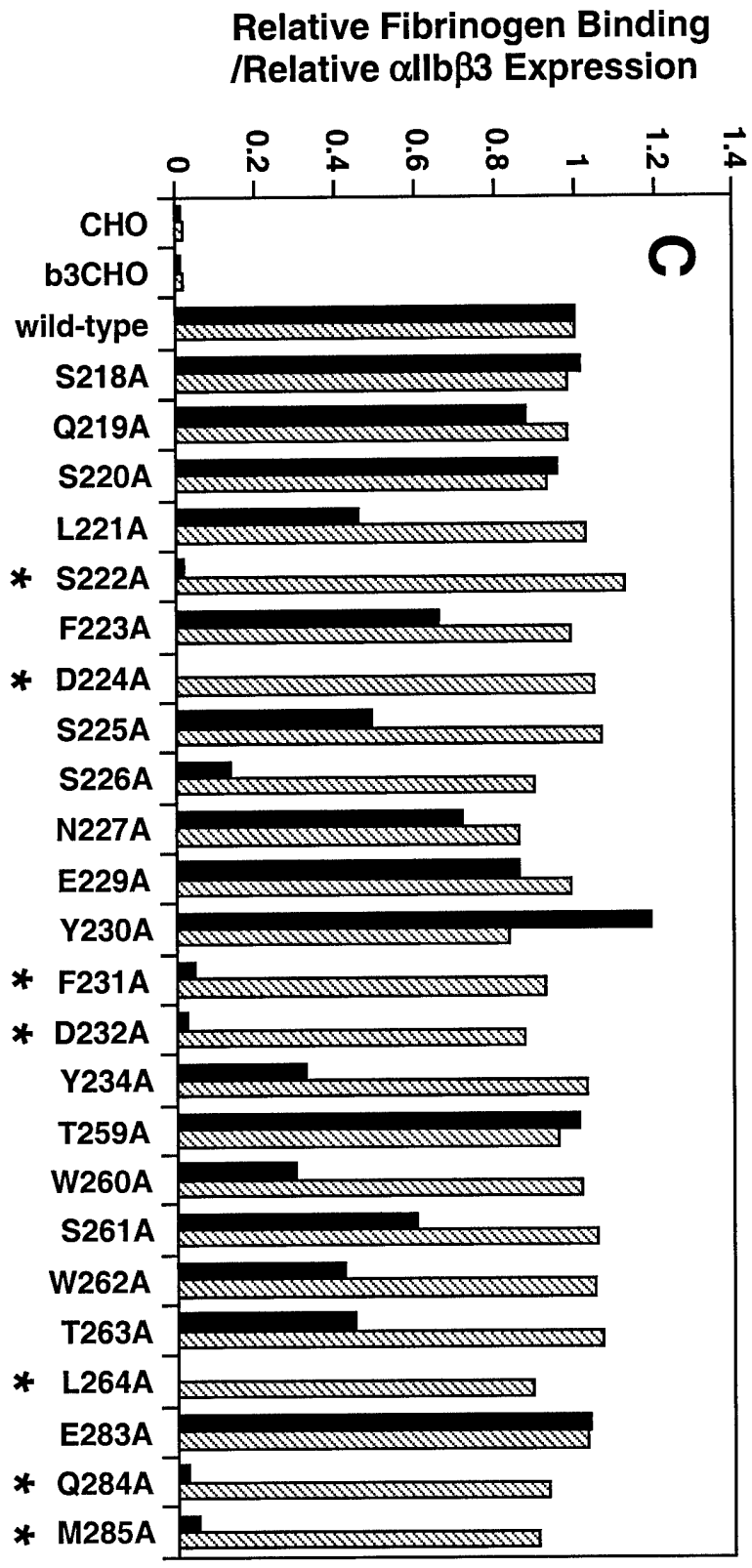
Relative Fibrinogen Binding
/Relative αIIbβ3 Expression
0
0.2
0.4
0.6
0.8
1
1.2
1.4
CHO
b3CHO
wild-type
S218A
Q219A
S220A
L221A
* S222A
F223A
* D224A
S225A
S226A
N227A
E229A
Y230A
* F231A
* D232A
Y234A
T259A
W260A
S261A
W262A
T263A
* L264A
E283A
* Q284A
* M285A
C

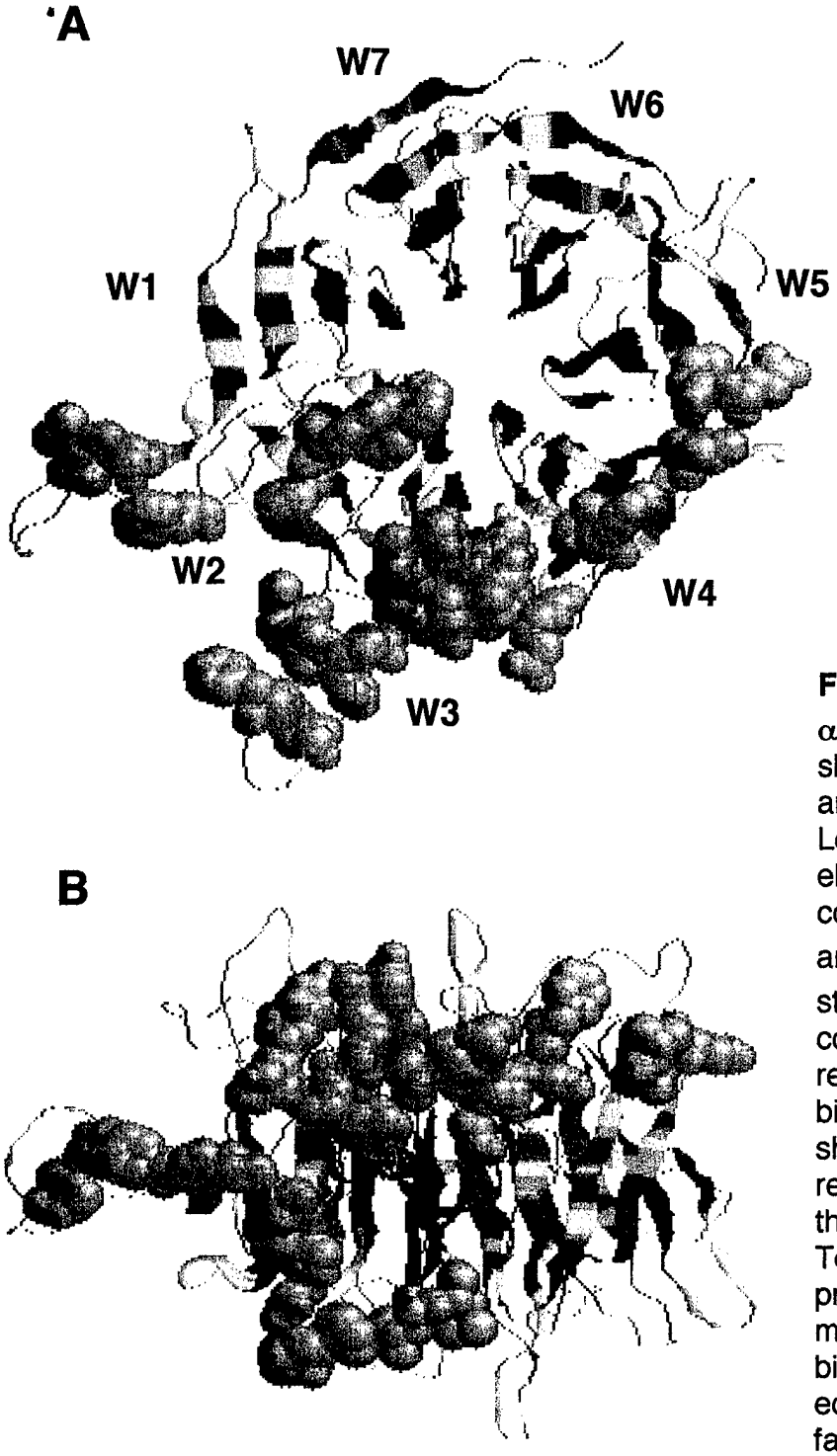

Fig. 3. The β-propeller model of αIIb. The seven four-stranded β-sheets (W) are arranged in a torus around a 7-fold pseudosymmetry axis. Loop swaps that did or did not eliminate fibrinogen binding are color coded as red and green, respectively and shown as ribbons. The outer β4 strand in β-sheet 3 (W3) is color coded as magenta. Amino acid residues that blocked fibrinogen binding when mutated to alanine are shown as spheres. The other residues that were not examined in this study are shown as blue ribbons. Top (A) and side (B) views of the propeller are shown. Note that mutations that eliminated fibrinogen binding are clustered in the top outer edge and side, but not in the bottom face of the propeller.

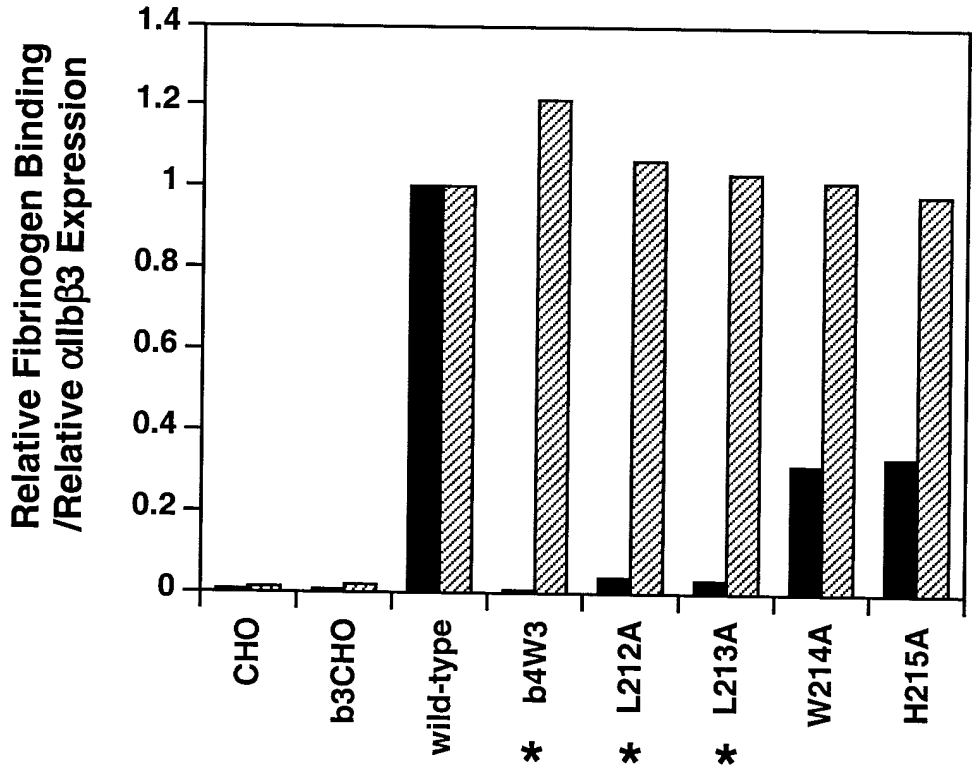

Fig. 4. Effect of mutations of β4-strand residues in β-sheet-3 on fibrinogen binding. Amino acid residues in the predicted β4 strand in β-sheet-3 of αIIb was swapped with homologous residues from α5. Individual amino acid residues within this region was mutated to Ala. The resulting β4W3 chimera and Ala mutants were transiently expressed in β3-CHO cells. Fibrinogen binding to cells expressing wt or mutant αIIbβ3 was examined as described in previous report. Relative fibrinogen binding (solid bar) and relative αIIbβ3 expression (hatchet bar) are shown. Mutants that exhibit fibrinogen binding less than 5 % of wild-type fibrinogen binding are marked with asterisks.

THE JOURNAL OF BIOLOGICAL CHEMISTRY
Vol. 274, No. 45, Issue of November 5, pp. 32108–32111, 1999
Printed in U.S.A.

Interaction between Collagen and the α_2 I-domain of Integrin $\alpha_2\beta_1$

CRITICAL ROLE OF CONSERVED RESIDUES IN THE METAL ION-DEPENDENT ADHESION SITE (MIDAS) REGION*

(Received for publication, March 31, 1999, and in revised form August 25, 1999)

Tetsuji Kamata, Robert C. Liddington‡, and Yoshikazu Takada§

From the Department of Vascular Biology, The Scripps Research Institute, La Jolla, California 92037 and ‡The Burnham Institute, La Jolla, California 92037

A docking model of the α_2 I-domain and collagen has been proposed based on their crystal structures (Emsley, J., King, S., Bergelson, J., and Liddington, R. C. (1997) *J. Biol. Chem.* 272, 28512–28517). In this model, several amino acid residues in the I-domain make direct contact with collagen (Asn-154, Asp-219, Leu-220, Glu-256, His-258, Tyr-285, Asn-289, Leu-291, Asn-295, and Lys-298), and the protruding C-helix of α_2 (residues 284–288) determines ligand specificity. Because most of the proposed critical residues are not conserved, different I-domains are predicted to bind to collagen differently. We found that deleting the entire C-helix or mutating the predicted critical residues had no effect on collagen binding to whole $\alpha_2\beta_1$, with the exception that mutating Asn-154, Asp-219, and His-258 had a moderate effect. We performed further studies and found that mutating the conserved surface-exposed residues in the metal ion-dependent adhesion site (MIDAS) (Tyr-157 and Gln-215) significantly blocks collagen binding. We have revised the docking model based on the mutagenesis data. In the revised model, conserved Tyr-157 makes contact with collagen in addition to the previously proposed Asn-154, Asp-219, His-258, and Tyr-285 residues. These results suggest that the collagen-binding I-domains (*e.g.* α_1, α_2, and α_{10}) bind to collagen in a similar fashion.

Several integrin α chains (α_1, α_2, α_{10}, α_L, α_M, α_X, α_D, and α_E) have inserted I- or A- domains of about 200 amino acid residues (1–11)). Integrins $\alpha_1\beta_1$ (1), $\alpha_2\beta_1$ (reviewed in Ref. 12), and $\alpha_{10}\beta_1$ (4) have been shown to bind to collagen and/or laminin. Several function-blocking antibodies map to the I-domains of $\alpha_2\beta_1$ (13) and $\alpha_1\beta_1$ (14). The recombinant α_2 I-domain fragment binds to collagen (15, 16), and the recombinant α_1 I-domain fragment binds to collagen and laminin (17). Conserved Asp and Thr residues in the α_2 I-domain (Asp-151, Thr-221, and Asp-254) are critical for collagen binding (15). These lines of evidence suggest that the I-domain is critically involved in collagen binding.

The crystal structures of the I-domains of the integrin α_M (18), α_L (19), and α_2 (20) subunits, and the A1 (21, 22) and A3 (23, 24) domains of von Willebrand factor (vWf)[1] have been published. This domain adopts a classic "Rossmann" fold and consists of a hydrophobic β-sheet in the middle and amphipathic α-helices on both sides. Interestingly, the integrin I-domain contains a Mg^{2+}/Mn^{2+} coordination site at its surface, which is not present in proteins with similar structures (*e.g.* the NAD binding domain of lactate dehydrogenase) or the vWf A1 and A3 domains (21–24). The Asp and Thr residues in α_2 that have been shown to be critical for ligand binding are involved in the coordination of a divalent cation in the crystal structure (20). The α_2 I-domain has a unique helix (the C-helix) protruding from the metal ion-dependent adhesion site (MIDAS) that creates a groove centered on the magnesium ion. Emsley *et al.* (20) proposed a model in which a collagen triple helix fits into the groove and a Glu side chain from collagen coordinates the metal ion. In this model, the C-helix is a major determinant for collagen binding. It was predicted that the following I-domain residues make direct contact with collagen: Asn-154 (the β_A-α_1 turn), Asp-219 and Leu-220 (the α_3-α_4 turn), Glu-256 and His-258 (the β_D-α_5 turn), and Tyr-285, Asn-289, Leu-291, Asn-295 and Lys-298 (the C-helix, α_6 and C-α_6 turn). However, these residues are not well conserved among collagen-binding I-domains (*e.g.* α_1, α_2, and α_{10}), suggesting that different I-domains interact with collagen in different manners. Here we show that mutation of the residues proposed to be critical for ligand binding or deletion of the entire C-helix did not significantly affect collagen binding to whole $\alpha_2\beta_1$ expressed on mammalian cells except for Asn-154, Asp-219, and His-258. In contrast, mutating several conserved MIDAS residues including Tyr-157 significantly blocks collagen binding. We have revised the docking model based on the mutagenesis data. In the revised model, interaction between the α_2 I-domain and collagen is mediated by relatively conserved residues in the MIDAS on the N-terminal side of the I-domain. Thus, it is suggested that the collagen-binding I-domains (*e.g.* α_1, α_2, and α_{10}) bind collagen in a similar fashion.

EXPERIMENTAL PROCEDURES

Monoclonal Antibodies—HAS-3 and HAS-4 (25) are generous gifts from F. Watt (Imperial Cancer Research Fund, London, UK.)

Adhesion of CHO Cells to Collagen—Wells of 96-well microtiter plates (Immulon-2, Dynatech Labs., Inc., Chantilly, VA) were coated with type I collagen (2 or 10 μg/ml) at 4 °C overnight. The other protein binding sites were blocked by incubating with 1% (w/v) bovine serum albumin (Calbiochem, CA) for 30 min at room temperature, and washing three times with phosphate-buffered saline (10 mM phosphate, 0.15 M NaCl, pH 7.4). Cells were harvested with 3.5 mM EDTA in phosphate-buffered saline and washed twice with Dulbecco's modified Eagle's medium. 10^5 cells (in 100 μl of Dulbecco's modified Eagle's medium) were added to each well and incubated for 1 h at 37 °C. The wells were rinsed three times with phosphate-buffered saline to remove unbound cells. Bound cells were quantified by assaying endogenous phosphatase activity (26).

Molecular Modeling—A model of a collagen triple helix was constructed from the crystal structure (Ref. 27, Protein Data Bank code

* This work was supported by National Institute of Health Grants GM47157 and GM49899 (to Y. T.) and by United States Department of the Army Grant DAMD17-97-1-7105 (to T. K.). This is publication Number 12010-VB from The Scripps Research Institute. The costs of publication of this article were defrayed in part by the payment of page charges. This article must therefore be hereby marked "*advertisement*" in accordance with 18 U.S.C. Section 1734 solely to indicate this fact.

§ To whom correspondence should be addressed: Dept. of Vascular Biology, VB-1, The Scripps Research Institute, 10550 North Torrey Pines Rd., La Jolla, CA 92037. Tel.: 619-784-7122; Fax: 619-784-7323; E-mail: takada@scripps.edu.

[1] The abbreviations used are: vWf, von Willebrand factor; MIDAS, metal ion-dependent adhesive site; CHO, Chinese hamster ovary.

1cag] as described previously (20). Side-chains from the sequence of the CB3(I)5/6 peptide containing the GER motif (28) were grafted onto the collagen in standard conformations using the program TOM (29). The glutamate of one of the GER motifs was attached to the Mg^{2+} ion of the MIDAS motif via one of its carboxylate oxygens at a distance of 2.0 Å. Keeping the I-domain fixed, the collagen was then allowed to rotate around a fixed point (the glutamate oxygen) to minimize the distance between the collagen and the side chains of those residues which showed reduced collagen binding when mutated and which were exposed on the surface of the I-domain. Unfavorably close contacts (<2.5 Å) between the collagen and the I-domain were monitored using the program TOM. Because the triple helical nature of collagen generates three chemically distinct strands even for a homo-tripeptide (which we call the leading, middle, and trailing strands) each of these was tested separately.

Other Methods—Swapping mutagenesis was carried out using the overlap extension polymerase chain reaction (30). The positions of the α_2 sequences replaced by homologous α_L sequences are residues 152–157, 212–219, and 257–262 (designated β_A-α_1, α_3-α_4, and β_D-α_5, respectively) (see Fig. 1). Deletion of residues 284–291 (designated α_C del) and point mutations were created by site-directed mutagenesis using the unique site elimination method with a double-stranded vector (31). The presence of mutation was confirmed by DNA sequencing. Transfection of cDNAs into CHO cells by electroporation, selection of transfected cells with G418, and flow cytometry were carried out as described previously (32).

RESULTS AND DISCUSSION

The MIDAS of the α_2 I-domain is composed of four loops (the β_A-α_1, α_3-α_4, β_D-α_5, and β_E-α_6 loops). The conserved residues Asp-151 in the β_A-α_1 loop, Thr-221 in the α_3-α_4 loop, and Asp-254 in the β_D-α_5 loop are critical for cation coordination and ligand binding (13, 15). A unique C-helix is inserted within the β_E-α_6 loop in the I-domains of the collagen-binding integrins α_1, α_2, and α_{10} but is not present in the I-domains of α_M or α_L, or the A_3 domain of vWf. This C-helix has been predicted to be a major determinant for collagen binding (20).

To identify the residues in the MIDAS that are critical for collagen binding, we introduced multiple point mutations into each MIDAS loop. We also included amino acid residues (Asn-154, Asp-219, Leu-220, Glu-256, His-258, Tyr-285, Asn-289, Leu-291, and Asn-295) that have been predicted to make direct contact with collagen (20). Mutant α_2 was transfected into CHO cells together with a neomycin-resistant gene and selected for G-418 resistance. Cells stably expressing the mutant α_2 were used for adhesion assays. Fig. 2 shows the adhesion of the mutants to collagen type I expressed as a percentage of cells adherent to collagen per percentage of human α_2 positive cells (normalized adhesion to collagen). We found that mutating several residues in the β_A-α_1 loop (Ser-153 and Tyr-157) and the α_3-α_4 loop (Gln-215) blocks collagen binding. In addition, mutation of Asn-154 and Ser-155 in the β_A-α_1 loop, Asp-219 in the α_3-α_4 loop, and His-258 in the β_D-α_5 loop produced an inhibitory effect at lower collagen coating concentrations.

We also swapped the β_A-α_1 (residues 152–157), α_3-α_4 (residues 212–219), and β_D-α_5 loops (residues 257–262) with the corresponding sequences of αL, which does not interact with collagen (Fig. 1). These swapping mutations did not change the conserved residues Asp-151, Thr-221, and Asp-254, which are critical for cation and collagen binding. Cells expressing mutant α_2 were tested for their ability to adhere to collagen. The expression of the α_3-α_4 swapping mutant was too low to produce reliable adhesion data (data not shown). Other mutants showed a surface-expression level comparable with that of wild type and reacted with multiple monoclonal antibodies against α_2 (Fig. 3a). The β_A-α_1 swapping mutant showed collagen binding at a background level. Also, the β_D-α_5 swapping mutant showed significantly reduced collagen binding. These results are consistent with those obtained using alanine-scanning mutagenesis.

In contrast, mutation of amino acid residues in the β_E-α_6 loop, including the C-helix, did not have any inhibitory effect on collagen binding. Mutation of Tyr-285, Asn-289, Leu-291, and Asn-295, which are predicted to make direct contact with collagen, did not significantly affect collagen binding, even at low (2 μg/ml) collagen coating concentrations (Fig. 2). It is possible that single amino acid substitution may not be enough to induce a detectable effect on collagen binding. So, we deleted most of the β_E-α_6 loop, including the entire C-helix, to determine whether the C-helix is critical for ligand specificity. These mutant α_2 cDNAs were stably expressed on CHO cells and further cloned to obtain high expressors. The α_C deletion mutant showed collagen binding at a level comparable with that of wild type (Fig. 3*A*). Adhesion of the α_C deletion mutant as a function of collagen coating concentration was tested. Adhesion to collagen of both wild type and α_C deletion mutant $\alpha_2\beta_1$ was saturated at about 1 μg/ml collagen coating concentration, indicating that the affinity to collagen is not affected by the α_C deletion (Fig. 3*B*).

These results suggest that collagen binding is mediated by relatively conserved MIDAS residues, which are located on the N-terminal side of the I-domain. Ser-153 and Ser-155 are involved in metal coordination, and mutating these residues would disrupt metal binding to the I-domain. Gln-215 is part of the MIDAS face and makes the main hydrogen bond to DXSXS loop. It is likely that mutating these residues blocks collagen

```
                          βA                  α1                  βB
a2-I   140 CPSL-IDVVVVCDESNSIYP--WDAVKNFLEKFVQGLDIGPTKTQVGLIQYANNP
aL-I   125 CIKGNVDLVFLFDGSMSLQPDEFQKILDFMKDVMKKL--SNTSYQFAAVQFSTSY
a1-I   143 CSTQ-LDIVIVLDGSNSIYP--WDSVTAFLNDLLKRMDIGPKQTQVGIVQYGENV
a10-I  140 CPTY-MDVVIVLDGSNSIYP--WSEVQTFLRRLVGKLFIDPEQIQVGLVQYGESP
vWFA3 1686 CSQP-LDVILLLDGSSSFPASYFDEMKSFAKAFISKANIGPRLTQVSVLQYGSIT
vWFA1 1272 CSRL-LDLVFLLDGSSRLSEAEFEVLKAFVVDMMERLRISQKWVRVAVVEYHDGS
aE-I   180     GTEIAIILDGSGSIDPPDFQRAKDFISNMMRNFYEKCFECNFALVQYGGVI
aM-I   128 CPQEDSDIAFLIDGSGSIIPHDFRRMKEFVSTVMEQL--KKSKTLFSLMQYSEEF
aX-I   126 CPRQEQDIVFLIDGSGSISSRNFATMMNFVRAVISQF--QRPSTQFSLMQFSNNF
aD-I   127 CPHQEMDIVFLIDGSGSIDQNDFNQMKGFVQAVMGQF--EGTDTLFALMQYSNLL

                    βC          α3                  α4
a2-I   192 RVVFNLNTYKTKEEMIVATSQTSQYGGDLTNTFGAIQYARKYAYSAASGGRRS-A
aL-I   178 KTEFDFSDYVKRKDPDALLKHVKHMLLLTNTFGAINYVATEVFREELGARPD-A
a1-I   195 THEFNLNKYSSTEEVLVAAKKIVQRGGRQTMTALGTDTARKEAFTEARGARRG-V
a10-I  192 VHEWSLGDFRTKEEVVRAAKNLSRREGRETKTAQAIMVACTEGFSQSHGGRPE-A
vWFA3 1740 TIDVPWNVVPEKAHLLSLVDVMQREGG-PSQIGDALGFAVRYLTSEMHGARPG-A
vWFA1 1326 HAYIGLKDRKRPSELRRIASQVKYAGSQVASTSEVLKYTLFQIF---SKIDRPEA
aE-I   232 QTEFDLRDFQDVMASLARVQNITQVGS-VTKTASAMQHVLDSIFTSSHGSRRK-A
aM-I   181 RIHFTFKEFQNNPNPRSLVKPITQLLG-RTHTATGIRKVVRELFNITNGARKN-A
aX-I   179 QTHFTFEEFRRTSNPLSLLASVHQLQG-FTYTATAIQNVVHRLFHASYGARRD-A
aD-I   180 KIHFTFTQFRTSPSQQSLVDPIVQLKG-LTFTATGILTVVTQLFHHKNGARKS-A

                    βD                  α5          βE      αC      α6
a2-I   246 TKVMVVVTDGESH--DGSMLKAVIDQCNHDNILRFGIAVLGYLNRNALDTKNLIK
aL-I   231 TKVLIIITDGEAT--DSGNIDAAK--DIIRYIIGIG-----KHFQTKESQE
a1-I   249 KKVMVIVTDGESH--DNHRLKKVIQDCEDENIQRFSIAILGSYNRQNLSTEQFVE
a10-I  246 ARLLVVVTDGESH--DGEELPAALKACEAGRVTRYGIAVLGHYLRRQRDPSSFLR
vWFA3 1793 SKAVVILVTDVSV--DS--VDAAADAARSNRVTVFPIGIG--------DR-YDAA
vWFA1 1378 SRIALLLMASQEPQRMSRNFVRYVQGLKKKKVIVIPVGIG-----PHAN----LK
aE-I   285 SKVMVVLTDGGIFE-DPLNLTTVINSPKMQGVERFAIGVG-----EEFKSARTAR
aM-I   234 FKILVVITDGEKFG-DPLGYEDVIPEADREGVIRYVIGVG-----DAFRSEKSRQ
aX-I   232 TKILIVITGDKKEG-DSLDYKDVIPMADAAGIIRYAIGVG-----LAFQNRNSWK
aD-I   233 KKILIVITDGQKYK-DPLEYSDVIPQAEKAGIIRYAIVGG-----HAFQGPTARQ

                        αF  βF      α7
a2-I   299 EIKAIA-SIPTERYFFNVSDEAALLEKAGTLGEQIFSIEG
aL-I   273 TLHKFA-SKPASEFVKILDTFEKLKDLFTELQKKIYVIEG
a1-I   302 EIKSIA-SEPPEKHFFNVSDELALVTTVKTLGERIFALEA
a10-I  299 EIRTIA-SDPDERFFFNVTDEAALTDIVDALGDRIFGLEG
vWFA3 1835 QLRILAGPAGDS-NVVKLQRIEDLPTMVTLGNSFLHKLC
vWFA1 1424 QIRLIEKQAPEN-KAFVLSSVDELEQQR---DEIVSYLC
aE-I   334 ELNLIA-SDPDETHAFKVTNYMALDGLLSKLRYNIISMEG
aM-I   283 ELNTIA-SKPPRDHVFQVNNFEALKTIQNQLREKIFAIEG
aX-I   280 ELNDIA-SKPSQEHIFKVEDFDALKDIQNQLKEKIFAIEG
aD-I   281 ELNTIS-SAPPQDHVFKVDNFAALGSIQKQLQEKIYAVEG
```

FIG. 1. **Residues/loops chosen for mutagenesis in this study.** The I-domains from integrin α_1, α_2, α_{10}, α_L, α_M, α_X, α_D, and α_E subunits and the vWf A1 and A3 domains were aligned. The β-strands and α-helices of the α_2 I-domain are *underlined*. Swapped regions of α_2 and α_L (β_A-α_1: 152–157; α_3-α_4: 212–219; β_D-α_5: 257–262) are outlined in the *box*. The deleted region in α_2 (αC del) is also *outlined*.

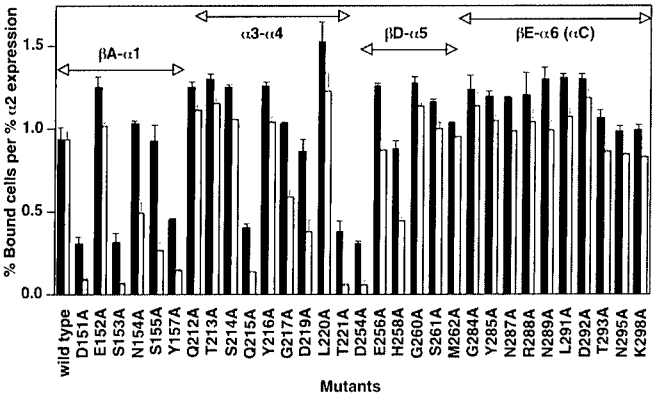

FIG. 2. **Effects of point mutations on collagen binding.** Cells stably expressing wild type or mutant α_2 were used to determine adhesion to collagen (at a 10 or 2 μg/ml coating concentration, *filled* column and *blank* column, respectively). Data are presented as percent bound cells to collagen per percent human α_2 positive cells to normalize α_2 expression. Typically 40–60% of cells are positive after selection with G-418. Previously published function-negative mutations (D151A, T221A, and D254A) are included as negative controls. These results suggest that several relatively conserved residues in the β_A-α_1, α_3-α_4, and β_D-α_5 loops are critical for collagen binding.

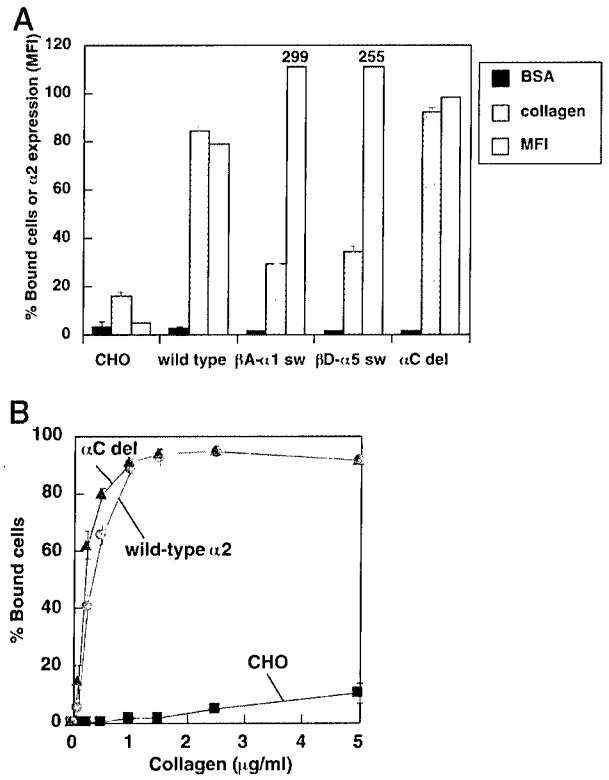

FIG. 3. **Effects of swapping/deletion mutations on collagen binding.** *A*, clonal CHO cells stably expressing wild type or mutant α_2 were incubated in the well coated with collagen type I or bovine serum albumin (negative control). After incubation at 37 °C for 1 h, nonadherent cells were removed and bound cells were determined by assaying endogenous phosphatase. Under the conditions used more than 80% of cells adhered to fibronectin as a positive control. *Solid bar*, *BSA*, bovine serum albumin; *hatched bar*, collagen; *MFI*, mean fluorescence intensity. *B*, adhesion to collagen of wild type and the α_C deletion mutant α_2 was determined as a function of collagen coating concentrations. The data suggest that the adhesive function of the α_C deletion mutant is comparable with that of wild type.

binding by disrupting metal binding to the I-domain. Asn-154, Asp-219, and His-258 have been predicted to make direct contact with collagen in the previous model (20), although the effects of mutating these residues are moderate. Tyr-157 is

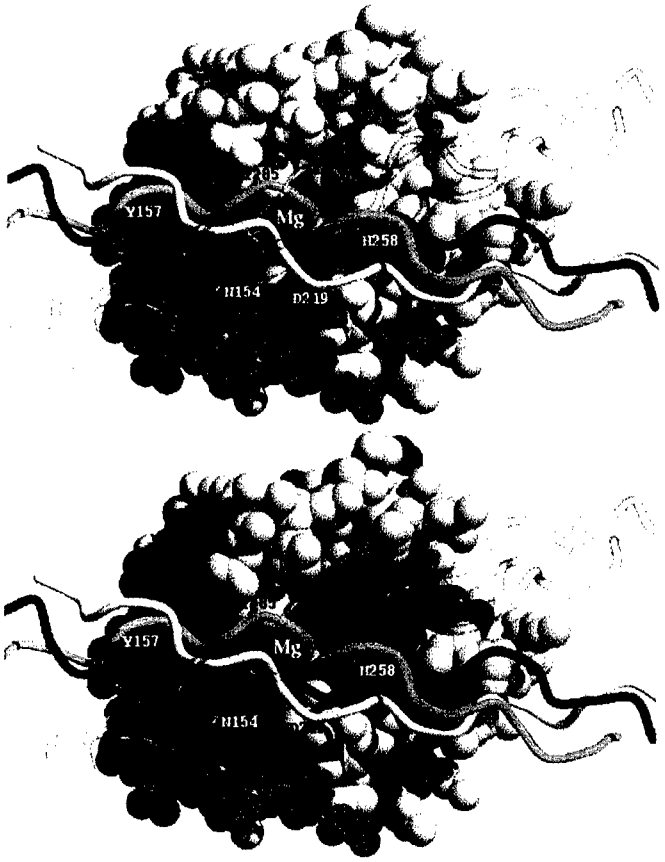

FIG. 4. **A revised docking model of the α_2 I-domain and collagen.** All-atom representation of the α_2 I-domain, viewed looking down onto the MIDAS face. In the *top panel*, residues with mutations that reduce collagen binding are in *red* (surface-exposed) or *pink* (likely to disrupt MIDAS). Residues with mutations that have no effect on collagen binding are in *cyan*. The Mg^{2+} ion is shown as a *gray ball*. The new collagen model is shown as a colored triple helical coil (*blue, green,* and *yellow*) drawn through the Cα positions. The previous model (20) is shown as a transparent triple helical coil. Certain residues referred to under "Results and Discussion" are labeled. In the *bottom panel*, residues shown in *red* are invariant between α_1, α_2, and α_{10} I-domains.

totally exposed to the surface, and this residue may make direct contact with collagen. Tyr-157 has not been predicted to make direct contact with collagen. Mutating the other residues that are predicted to be critical for collagen binding in the proposed model (Leu-220, Glu-256, Tyr-285, Asn-289, Leu-291, Asn-295, and Lys-298) has no significant effect on collagen binding. Even deletion of the entire C-helix did not significantly affect collagen binding. These results support the role of the MIDAS motif in collagen binding because many of the mutants that affect collagen binding are predicted to disrupt the MIDAS motif. However, the present results are not fully consistent with the proposed model for collagen/α_2 I-domain binding (20).

We have modified the collagen/α_2 I-domain docking model based on the present mutagenesis data (Fig. 4). Recently, short synthetic triple-helical peptide corresponding to residues 502–516 of the collagen type I α_1 chain, has been shown to bind to purified $\alpha_2\beta_1$ and recombinant α_2 I-domain (28). The Glu and Arg residues in the GER triplet were found to be essential for recognition by α_2 I-domain (28). In the current model, we first attached the glutamate side chain of the GER motif to the MIDAS Mg^{2+} ion. We then rotated the collagen to minimize the distance between the collagen and those surface-exposed residues implicated in collagen binding (His-258, Tyr-157, Asp-219, and Asn-154) while maintaining the 2-Å bond between the

glutamate oxygen and the Mg^{2+} ion and avoiding other close contacts (<2.5 Å) with the protein. It was not initially possible to make favorable hydrogen bonds with all four side chains simultaneously, so the side chains were allowed to rotate about their Cα-Cβ bonds to make plausible hydrogen bonds with the collagen backbone carbonyl oxygens and amide nitrogens. The collagen orientation was then refined to optimize the hydrogen bonding geometry. This procedure allowed all four I-domain side chains to make reasonable hydrogen bonds to the collagen. This model predicts that the side chain of Tyr-285, which projects from the C helix into the groove, makes unavoidable contact with the collagen and that further hydrogen bonds can be made between the Tyr hydroxyl and the collagen main chain. This revised model, which is rotated about 30 degrees from the previously published model, allows the arginine from the GER motif of the preceding strand to make a salt bridge to Glu-256. The previous model would not allow enough space for the arginine side chain without imposing unfavorable side chain torsion angles. Because mutation of Glu-256 does not significantly block collagen binding in the present study, this salt bridge might not be energetically important. The triple helical character of a symmetric collagen trimer generates three chemically distinct strands, which we call the leading, middle, and lagging strands. Attaching either the leading or middle strand glutamate to the Mg^{2+} ion leads to the same conclusions. Attaching the trailing strand makes a difference because there is no arginine from the preceding strand to form a salt-bridge to Glu-256. The alternative orientation with the collagen rotated by 180 degrees is much less favorable because the arginine of the GER motif would clash sterically with the I-domain. As pointed out in our previous model, an aspartic acid side chain in place of the GER glutamate would be too short to reach the Mg^{2+} ion without creating a large number of steric clashes. Because Asn-154, Tyr-157, His-258 are conserved in other collagen-binding integrin I-domains (α_1 and α_{10}), it is reasonable to assume that these residues are also involved in collagen binding in these integrins (Fig. 4). This model is consistent with the observation that tyrosine and arginine are enriched in hot spots of binding energy in the protein-protein interface (33).

In the present model, the highly conserved D151 and D254 residues in the α_2 I-domain are buried underneath the Mg^{2+} ion and cannot contact collagen directly. We have reported that mutating these residues only partially affects collagen binding to the recombinant α_2 I-domain fragment (13, 15). Also, Bienkowska *et al.* (23) reported that mutating the corresponding residues in the recombinant fragment of the vWf A3 domain does not affect collagen binding. However, the same mutation in the whole α_2 molecule completely blocks collagen binding to $\alpha_2\beta_1$ (13, 15). It is possible that cation coordination through these residues is critical for ligand binding in the I-domain of the integrin molecule but not in similar domains in non-integrin structures (*e.g.* vWf). Consistently, the cation-binding site is not present in the vWf A3 domain (23, 24). Further studies would be needed to clarify the role of the conserved Asp residues in integrin I-domains. Several other collagen-binding sites have been reported. A collagen binding surface on osteonectin has been mapped by mutagenesis: it consists of a flat surface 15 Å in diameter containing polar and apolar residues (34), a crucial arginine residue, and intriguingly a Ca^{2+} binding site that might be directly involved in collagen binding. Docking and mutagenesis of *Staphylococcus aureus* adhesin identified another crucial arginine and a narrow groove as the binding site for collagen (35). The collagen binding surface on vWF-A3 has not been mapped but the structurally analogous surface lacks the charged residues found in the integrin I-domains (23, 24). Further studies will be required to determine whether there are any common collagen binding mechanisms.

While this paper was under review, the crystal structure of a GER-containing collagen peptide/α_2 I domain complex has been solved.[2] Preliminary analysis reveals that the structure is very similar to the revised model described here. Thus, the orientation and location of the collagen is as predicted, with Glu residues from the collagen coordinating directly to the metal ion. In addition, there is an unexpected change in the C helix so that it no longer touches the collagen, in agreement with the mutagenesis results.

Acknowledgments—We thank F. Watt for antibodies and M. Cruz for sharing unpublished data. We also thank K. K. Tieu and W. Puzon-McLaughlin for excellent technical assistance.

REFERENCES

1. Ignatius, M. J., Large, T. H., Houde, M., Tawil, J. W., Burton, A., Esch, F., Cabonetto, S., and Reichardt, L. F. (1990) *J. Cell Biol.* **111,** 709–720
2. Briesewitz, R., Epstein, M. R., and Marcantonio, E. E. (1993) *J. Biol. Chem.* **268,** 2989–2996
3. Takada, Y., and Hemler, M. E. (1989) *J. Cell Biol.* **109,** 397–407
4. Camper, L., Hellman, U., and Lundgren-Akerlund, E. (1998) *J. Biol. Chem.* **273,** 20383–20389
5. Larson, R., Corbi, A. L., Berman, L., and Springer, T. A. (1989) *J. Cell Biol.* **108,** 703–712
6. Corbi, A. L., Kishimoto, T. K., Miller, L. J., and Springer, T. A. (1988) *J. Biol. Chem.* **263,** 12403–12411
7. Arnaout, M. A., Gupta, S. K., Pierce, M. W., and Tenen, D. G. (1988) *J. Cell Biol.* **106,** 2153–2158
8. Pytela, R. (1988) *EMBO J.* **7,** 1371–1378
9. Corbi, A. L., Miller, L. J., O'Connor, K., Larson, R. S., and Springer, T. A. (1987) *EMBO J.* **6,** 4023–4028
10. Van der Vieren, M., Trong, H. L., Wood, C. L., Moore, P. F., St. John, T., Staunton, D. E., and Gallatin, W. M. (1995) *Immunity* **3,** 683–690
11. Shaw, S. K., Cepek, K. L., Murphy, E. A., Russell, G. L., Brenner, M. B., and Parker, C. M. (1994) *J. Biol. Chem.* **269,** 6016–6025
12. Santoro, S. A., and Zutter, M. M. (1995) *Thromb. Haemostasis* **74,** 813–821
13. Kamata, T., Puzon, W., and Takada, Y. (1994) *J. Biol. Chem.* **269,** 9659–9663
14. Kern, A., Briesewitz, R., Bank, I., and Marcantonio, E. (1994) *J. Biol. Chem.* **269,** 22811–22816
15. Kamata, T., and Takada, Y. (1994) *J. Biol. Chem.* **269,** 26006–26010
16. Tuckwell, D., Calderwood, D. A., Green, L. J., and Humphries, M. J. (1995) *J. Cell Sci.* **108,** 1629–1637
17. Calderwood, D. A., Tuckwell, D. S., Eble, J., Kuhn, K., and Humphries, M. J. (1997) *J. Biol. Chem.* **272,** 12311–12317
18. Lee, J.-O., Rieu, P., Arnaout, M. A., and Liddington, R. (1995) *Cell* **80,** 631–638
19. Qu, A., and Leahy, D. (1995) *Proc. Natl. Acad. Sci. U. S. A.* **92,** 10277–10281
20. Emsley, J., King, S. L., Bergelson, J. M., and Liddington, R. C. (1997) *J. Biol. Chem.* **272,** 28512–28517
21. Emsley, J., Cruz, M., Handin, R., and Liddington, R. (1998) *J. Biol. Chem.* **273,** 10396–10401
22. Celikel, R., Varughese, K. I., Madhusudan, Yoshioka, A., Ware, J., and Ruggeri, Z. M. (1998) *Nat. Struct. Biol.* **5,** 189–194
23. Bienkowska, J., Cruz, M., Atiemo, A., Handin, R., and Liddington, R. (1997) *J. Biol. Chem.* **272,** 25162–25167
24. Huizinga, E. G., Martijn van der Plas, R., Kroon, J., Sixma, J. J., and Gros, P. (1997) *Structure* **5,** 1147–1156
25. Tenchini, M. L., Adams, J. C., Gilbert, C., Steel, J., Hudson, D. L., Malcovati, M., and Watt, F. M. (1993) *Cell Adhesion Comm.* **1,** 55–66
26. Prater, C. A., Plotkin, J., Jaye, D., and Frazier, W. A. (1991) *J. Cell Biol.* **112,** 1031–1040
27. Bella, J., Eaton, M., Brodsky, B., and Berman, H. M. (1994) *Science* **266,** 75–81
28. Knight, C. G., Morton, L. F., Onley, D. J., Peachey, A. R., Messent, A. J., Smethurst, P. A., Tuckwell, D. S., Farndale, R. W., and Barnes, M. J. (1998) *J. Biol. Chem.* **273,** 33287–33294
29. Cambillau, C., Horjales, E., and Jones, T. A. (1984) *J. Mol. Graphics* **2,** 53–54
30. Horton, R. M., and Pease, L. R. (1991) in *Directed Mutagenesis; A Practical Approach* (McPherson, M. J., ed), pp. 217–247, IRL Press, Oxford
31. Deng, W. P., and Nickoloff, J. A. (1992) *Anal. Biochem.* **200,** 81–88
32. Takada, Y., Ylanne, J., Mandelman, D., Puzon, W., and Ginsberg, M. (1992) *J. Cell Biol.* **119,** 913–921
33. Bogan, A. A., and Thorn, K. S. (1998) *J. Mol. Biol.* **280,** 1–9
34. Sasaki, T., Hohenester, E., Gohring, W., and Timpl, R. (1998) *EMBO. J* **17,** 1625–1634
35. Symersky, J., Patti, J. M., Carson, M., House-Pompeo, K., Teale, M., Moore, D., Jin, L., Schneider, A., DeLucas, L. J., Hook, M., and Narayana, S. V. (1997) *Nat. Struct. Biol.* **4,** 833–838

[2] J. Emsley, C. G. Knight, M. J. Barnes, R. W. Farndale, and R. Liddington, unpublished results.

THE JOURNAL OF BIOLOGICAL CHEMISTRY
Vol. 275, No. 11, Issue of March 17, pp. 7795–7802, 2000
Printed in U.S.A.

Multiple Discontinuous Ligand-mimetic Antibody Binding Sites Define a Ligand Binding Pocket in Integrin $\alpha_{IIb}\beta_3$*

(Received for publication, September 28, 1999, and in revised form, November 17, 1999)

Wilma Puzon-McLaughlin, Tetsuji Kamata, and Yoshikazu Takada‡

From the Department of Vascular Biology, The Scripps Research Institute, La Jolla, California 92037

Integrin $\alpha_{IIb}\beta_3$, a platelet fibrinogen receptor, is critically involved in thrombosis and hemostasis. However, how ligands interact with $\alpha_{IIb}\beta_3$ has been controversial. Ligand-mimetic anti-$\alpha_{IIb}\beta_3$ antibodies (PAC-1, LJ-CP3, and OP-G2) contain the RGD-like RYD sequence in their CDR3 in the heavy chain and have structural and functional similarities to native ligands. We have located binding sites for ligand-mimetic antibodies in α_{IIb} and β_3 using human-to-mouse chimeras, which we expect to maintain functional integrity of $\alpha_{IIb}\beta_3$. Here we report that these antibodies recognize several discontinuous binding sites in both the α_{IIb} and β_3 subunits; these binding sites are located in residues 156–162 and 229–230 of α_{IIb} and residues 179–183 of β_3. In contrast, several nonligand-mimetic antibodies (*e.g.* 7E3) recognize single epitopes in either subunit. Thus, binding to several discontinuous sites in both subunits is unique to ligand-mimetic antibodies. Interestingly, these binding sites overlap with several (but not all) of the sequences that have been reported to be critical for fibrinogen binding (*e.g.* N-terminal repeats 2–3 but not repeats 4–7, of α_{IIb}). These results suggest that ligand-mimetic antibodies and probably native ligands may make direct contact with these discontinuous binding sites in both subunits, which may constitute a ligand-binding pocket.

Integrin $\alpha_{IIb}\beta_3$ is a platelet fibrinogen receptor that is critically involved in platelet aggregation (1). Thus $\alpha_{IIb}\beta_3$-fibrinogen interaction is a therapeutic target for thrombosis and hemostasis. However, how ligands interact with the integrin α_{IIb} and β_3 subunits has been the subject of much discussion.

The α_{IIb} subunit has seven repeated sequences of 60–70 residues each in its N-terminal portion. Two different regions of the α_{IIb} subunit have been implicated in ligand binding. The second metal binding site of α_{IIb} (residues 294–314 in N-terminal repeat 5 of α_{IIb}) has been identified as a ligand binding site by chemically cross-linking the γ-peptide (HHLGGAKQ-AGDV$^{400-411}$) of the fibrinogen γ chain C-terminal domain (2). Both the peptide derived from this α_{IIb} sequence and its antibodies have been shown to block fibrinogen binding to $\alpha_{IIb}\beta_3$ (3). Consistently, recombinant bacterial proteins that consist of repeats 4–7 of α_{IIb} (residues 171–464) have been shown to bind to ligands in a cation-dependent manner (4). On the other hand, alanine-scanning mutagenesis (5)[1] suggests that the predicted loops in repeats 2 and 3 are critical for ligand binding. Also, function-blocking anti-$\alpha_{IIb}\beta_3$ monoclonal antibodies (mAbs)[2] are mapped in repeats 2 and 3 (5).[1] It has not been established which regions of α_{IIb} actually interact with ligands.

The presence of an I-domain-like structure within the β subunit has been suggested based on the similarity in hydropathy profiles between the I-domain of the α_M subunit and part of the β subunit (6). The N-terminal region of the β_3 subunit has components that are critical for ligand binding and its regulation (reviewed in Ref. 7). The RGD-containing peptide chemically cross-links to the N-terminal region (residues 109–171) of the β_3 subunit (8). Several different β_3 sequences, MDLSYSMKDDLWSI (residues 118–131) (9), DDLW (residues 126–129 of β_3) (10), DAPEGGFDAIMQATV (residues 217–231 of β_3) (11, 12), and VSRNRDAPEG (residues 211–221 of β_3) (13, 14) have been implicated in ligand interaction. The disulfide-linked CYDMKTTC sequence (residues 177–184 in β_3) in a large predicted loop is critical for the ligand specificity of $\alpha_v\beta_3$ (15). There are several residues that are critical for ligand binding in the putative I-domain-like structure of β subunits (16–22). These critical oxygenated residues are located in several separate predicted loop structures within the I-domain-like structure of the β subunit (15). It has not been established how these predicted loops, which are critical for ligand binding and specificity, are organized. Two distinct models of the putative I-domain-like structure of β subunits have been published based on the structure of the β_M I-domain (21, 23). It has also been proposed that there is no I-domain-like structure in the β_3 subunit (24).

Three anti-human $\alpha_{IIb}\beta_3$-specific mAbs, PAC-1 (25), OP-G2 (26), and LJ-CP3 (27), have the tripeptide RYD sequence that mimics the RGD sequence in the CDR3 region of the heavy chain. These mAbs inhibit both fibrinogen binding to platelets and fibrinogen-dependent aggregation of platelets. Binding of these mAbs is cation-dependent and is completely blocked by RGD-containing peptides. PAC-1 does not bind to nonactivated platelets (25). OP-G2 and LJ-CP3 can bind to nonactivated $\alpha_{IIb}\beta_3$, but this binding increases upon activation. The ligand-mimetic properties of these mAbs suggest that they have structural and functional similarities to ligands (*e.g.* fibrinogen). Structure-function studies of these mAbs indicate that the RYD sequence in the CDR3 in their heavy chain occupies the same space as RGD does in conformationally constrained, bioactive $\alpha_{IIb}\beta_3$ ligands (28).

In the present study, to clarify the controversies surrounding

* This work was supported by National Institute of Health Grants GM47157 and GM49899 (to Y. T.) and by Department of the Army Grant DAMD17-97-1-7105 (to T. K.). This is Publication #12252-VB from The Scripps Research Institute. The costs of publication of this article were defrayed in part by the payment of page charges. This article must therefore be hereby marked "*advertisement*" in accordance with 18 U.S.C. Section 1734 solely to indicate this fact.

The nucleotide sequence(s) reported in this paper has been submitted to the GenBank™/EBI Data Bank with accession number(s) AF166384 (mouse integrin αIib).

‡ To whom correspondence should be addressed: Dept. of Vascular Biology, CAL-10, The Scripps Research Institute, 10550 N. Torrey Pines Rd., La Jolla, CA 92037. Tel.: 858-784-7636; Fax: 858-784-7645; E-mail: takada@scripps.edu.

[1] T. Kamata, K. K. Tieu, A. Irie, T. A. Springer, and Y. Takada, unpublished data.

[2] The abbreviations used are: mAb monoclonal antibody; CHO, Chinese hamster ovary; FITC, fluorescein isothiocyanate; PE, phycoerythrin.

$\alpha_{IIb}\beta_3$-ligand interaction, we studied how ligand-mimetic mAbs as model ligands recognize α_{IIb} and β_3. We found that these mAbs uniquely recognize several discontinuous binding sites in both α_{IIb} and β_3. These binding sites overlap with several (but not all) of the sequences that have previously been reported to be critical for fibrinogen binding (*e.g.* N-terminal repeats 2–3, but not repeats 4–7, of α_{IIb}). These results strongly suggest that native ligands make direct contact with these discontinuous binding sites, which may constitute a ligand binding pocket at the α/β boundary.

EXPERIMENTAL PROCEDURES

Monoclonal Antibodies and cDNAs

The specificities of the mAbs used in this study are shown in Table I. mAbs 15 and D57 (29) are a kind gift from M. H. Ginsberg (The Scripps Research Institute). AP-2 (30) is from T. Kunicki (The Scripps Research Institute). 2G12 (31) is from V. Woods (University of California San Diego, San Diego, CA). PL98DF6 (32) is from J. Ylanne (University of Helsinki, Helsinki, Finland). PAC-1 and AZA9 (52) are from S. J. Shattil (The Scripps Research Institute). OP-G2 (33) is from S. Tomiyama (Osaka University, Osaka, Japan). LJ-CP3, LJ-CP8 and LJ-P9 (27) are from Z. M. Ruggeri (The Scripps Research Institute). PT25-2 (34) is from M. Handa and Y. Ikeda (Keio University, Tokyo, Japan). 16N7C2 (35) is from H. Deckmyn (Center for Molecular and Vascular Biology, Leuven, Belgium). 7E3 (36) is a kind gift of B. S. Coller (Mount Sinai Hospital, New York). LM609 (37) is a kind gift of D. Cheresh (The Scripps Research Institute).

Methods

Construction and Transfection of cDNAs for Human α_{IIb} and β_3 Mutants—Human α_{IIb} and β_3 cDNAs were obtained from J. C. Loftus (The Scripps Research Institute). The mouse α_{IIb} cDNA clone from the mouse EST data base was obtained from American Type Culture Collection (clone 1498358) and partially sequenced by ABI automatic sequencer at the Scripps protein and nucleic acid core facility (GenBank™ accession number AF166384). Wild-type human α_{IIb} and β_3 cDNAs were subcloned into pBJ-1 vector. Site-directed mutagenesis was carried out as described (38). The presence of the mutation was verified by DNA sequencing. Wild-type and mutant α_{IIb} cDNA constructs in pBJ-1 vector were transfected by electroporation into CHO (Chinese hamster ovary) cells (1×10^7 cells) homogeneously expressing human β_3 (β_3-CHO) or into parent untransfected CHO cells together with wild-type human β_3 cDNA in pBJ-1, as described previously (5). We obtained essentially the same results either way. Wild-type and mutant β_3 cDNAs were transfected into CHO-K1 cells together with wild-type α_{IIb} cDNA. Cells were harvested 48 h after transfection and used for antibody and/or fluorescein isothiocyanate (FITC)-labeled fibrinogen and PAC-1 binding assays. Mouse α_{IIb} cDNA encoding the N-terminal 443 residues was fused to the human α_{IIb} cDNA using an *Nhe*I site after the *Nhe*I site was introduced into the human α_{IIb} cDNA at the corresponding position.

Binding of FITC-labeled Fibrinogen and mAb PAC-1 to CHO Cells—Fibrinogen (Enzyme Research Laboratories, South Bend, IN) was labeled with FITC as described previously (39, 40). mAb PAC-1 was labeled with FITC essentially as described (41). Fibrinogen binding to cells transiently expressing $\alpha_{IIb}\beta_3$ was determined as described previously (42) with some modifications. Briefly, cells were first incubated with PL98DF6 followed by phycoerythrin (PE)-conjugated anti-mouse IgG (BIOSOURCE, Camarillo, CA). After washing, cells were incubated with FITC-labeled fibrinogen or PAC-1 in the presence of control mouse IgG or PT25-2 in 5 mM Hepes/Tyrode, 2 mM Ca^{2+}, and 2 mM Mg^{2+} buffer, pH 7.4. Binding of FITC-labeled fibrinogen or PAC-1 to PE-labeled cells expressing high level $\alpha_{IIb}\beta_3$ was examined in FACScan.

Flow Cytometry—Flow cytometric analysis was performed as described (43). To normalize the data for $\alpha_{IIb}\beta_3$ expression, % expression of each binding site in mutant α_{IIb} was first normalized using % α_{IIb} expression with mAb PL98DF6 for $\alpha_{IIb}\beta_3$ complex-specific mAbs. For the anti-β_3 mAbs 7E3 and 16N7C2, % expression of each binding site in mutant α_{IIb} was first normalized using % β_3 expression with mAb 15 (normalized % expression). Data is shown as the normalized % of expression in mutants relative to wild-type. Binding sites for mAbs PL98DF6 and 15 were not found in the α_{IIb} and β_3 regions tested in this study (data not shown).

TABLE I
mAbs used in this study

mAbs	Specificity	Characteristics
LJ-CP3, OP-G2, PAC-1	$\alpha_{IIb}\beta_3$	Ligand-mimetic, the RYD motif in the heavy chain CDR3
16N7C2	β_3	Inhibitory, the RGD motif in the heavy chain CDR3
7E3	β_3	Inhibitory
2G12, A2A9, AP-2, LJ-CP8, LJ-P9	$\alpha_{IIb}\beta_3$	Inhibitory
PT25–2	$\alpha_{IIb}\beta_3$	Activating
D57	$\alpha_{IIb}\beta_3$	Nonfunctional
LM609	$\alpha_v\beta_3$	Inhibitory
PL98DF6	α_{IIb}	Nonfunctional
15	β_3	Nonfunctional

RESULTS

Ligand-mimetic mAbs Recognize Several Discontinuous N-terminal Regions of the α_{IIb} Subunit—We used human-to-mouse α_{IIb} and β_3 mutations to localize binding sites for three ligand-mimetic mAbs and several function-blocking or -activating mAbs (Table I). The rationale behind this strategy is that all of the mAbs used in this study recognize human $\alpha_{IIb}\beta_3$ but not mouse $\alpha_{IIb}\beta_3$. We also expect this strategy to enable for us to maintain the ligand binding function of the mutants while eliminating the potential problems associated with mutation of individual residues to Ala, which could indirectly induce conformational changes.

Since the mouse α_{IIb} sequence has not been published, we first sequenced the N-terminal region of putative mouse α_{IIb} cDNA clones from the mouse EST cDNA data base (Fig. 1*a*). The N-terminal seven-repeat region of human α_{IIb} is 82.5% identical to that of mouse α_{IIb} (they have 452 and 451 amino acid residues, respectively). To determine whether binding sites for ligand-mimetic and nonligand-mimetic mAbs are located in the seven-repeat region of α_{IIb}, we first replaced N-terminal 443 amino acid residues of human α_{IIb} with the corresponding sequence of mouse α_{IIb}. The human/mouse α_{IIb} chimera was transiently transfected into β_3-CHO cells that homogeneously express wild-type human β_3. Reactivity of the transfected cells to a panel of mAbs is shown in Table II. The results indicate that the anti-$\alpha_{IIb}\beta_3$ mAbs tested recognize $\alpha_{IIb}\beta_3$ but not $\alpha_v\beta_3$. All of the $\alpha_{IIb}\beta_3$ mAbs tested, except for AP-2 and D57, require the N-terminal 443-amino acid residues of human α_{IIb} for $\alpha_{IIb}\beta_3$ recognition. AP-2 and D57 require the α_{IIb} subunit but do not require the human N-terminal 443 residues. The anti-α_{IIb} mAb PL98DF6 does not require the human N-terminal 443 residues.

We introduced human-to-mouse mutations, alone or in groups, into the N-terminal seven-repeat region of human α_{IIb} to identify α_{IIb} sequences that are critical for antibody binding (Fig. 1*a*). The human-to-mouse α_{IIb} mutants were individually transfected into β_3-CHO cells. The capacity of transiently expressed $\alpha_{IIb}\beta_3$ mutants to bind to a panel of mAbs (listed in Table I) was tested using flow cytometry. Fig. 2 shows flow cytometric profiles of wild-type $\alpha_{IIb}\beta_3$ and the A16 mutant (V156A/N158S/D159 deletion/S161R/W162G) as an example. 30–50% of cells transfected with wild-type $\alpha_{IIb}\beta_3$ are positive with LJ-CP3, OP-G2, and PT25-2. 30–50% of cells expressing the A16 mutant are positive with PT25-2, but almost none of them are positive with LJ-CP3 and OP-G2. This indicates that the mutant is expressed on the cell surface but does not react with LJ-CP3 and OP-G2.

The results for 36 mutants are summarized in Table III (data is shown only for selected mutants). Because expression levels vary, we normalized the percentage of positive cells for each mutant. We used PL98DF6 (an anti-α_{IIb} mAb) to normalize the $\alpha_{IIb}\beta_3$ expression and mAb 15 (an anti-β_3 mAb) to normalize

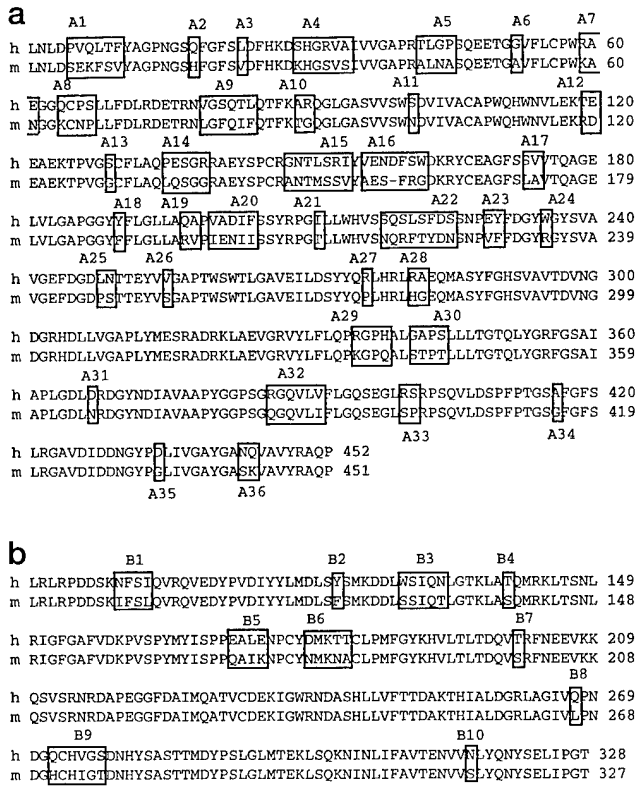

FIG. 1. **Alignment of human and mouse α_{IIb} (*a*) and β_3 (*b*) subunits.** *a*, in the N-terminal seven-repeat regions of human (*h*) and mouse (*m*) α_{IIb}, the amino acid sequences are different at 79 positions. Human-to-mouse mutations alone or in groups (36 total) were introduced and designated A1-36. Positions of mutations in the human-to-mouse α_{IIb} mutants are *A1*, P5S/V6E/Q7K/L8F/T9S/F10V; *A2*, Q18H; *A3*, L23V; *A4*, S29K/R32S/A34S; *A5*, T42A/G44N/P45A; *A6*, G52A; *A7*, R59K/E61N; *A8*, Q64K/P66N/S67P; *A9*, V79L/S81F/T83I/L84F; *A10*, A89T/R90G; *A11*, S101N; *A12*, T119R/E120D; *A13*, S129G; *A14*, P135L/E136Q/R139G; *A15*, G148A/L151M/R153S/I154V; *A16*, V156A/N158S/D159 deletion/S161R/W162G; *A17*, S173L/V174A; *A18*, Y190F; *A19*, Q197R/A198V; *A20*, V200I/A201E/D202N/F204I/S206T; *A21*, I211T; *A22*, S218N/S220R/L221F/S222T/F223Y/S225N; *A23*, E229V/Y230F; A24, W235R; *A25*, L248P/N249S; *A26*, V255S; *A27*, R276P; *A28*, R281H/A282G; *A29*, R335K/H338Q; *A30*, G341S/A342T/S344T; *A31*, D367N; *A32*, R386E/V391I; *A33*, R400S/S401P; *A34*, A416G; *A35*, D434G; and *A36*, N443S/Q444K. *b*, the amino acid sequences of human and mouse β_3 are different at 17 positions. Human-to-mouse mutations, alone or in groups (10 total), were introduced and designate B1-10. Positions of mutations in the human-to-mouse β_3 mutants are *B1*, N99I/I102L; *B2*, Y122F; *B3*, W129S/N133T; *B4*, T140S; *B5*, E171Q/L173I/E174K; *B6*, D179N/T182N/T183A; *B7*, T201S; B8, Q267L; *B9*, Q272H/V275I/S277T; and *B10*, N316S.

the β_3 expression. Data are presented as the ratio of the mutant cells that are positive to mAbs to the wild-type cells that are positive to mAbs. We found that LJ-CP3 binding is completely blocked by the A16 mutation and almost completely blocked by the A23 mutation (E229V/Y230F). OP-G2 binding is almost completely blocked by the A16 mutation. Binding of nonligand-mimetic function-blocking mAbs LJ-P9 and LJ-CP8 is completely blocked by the A9 mutation (V79L/S81F/T83I/L84P) and by the A16 mutation, respectively. Binding of activating mAb PT25-2 was completely blocked by the A29 (R335K/H338Q) mutation. 32 other mutations (listed in Fig. 1*a* and its legend) did not significantly affect the binding of the mAbs tested. The A16 mutation blocks binding of LJ-CP3, OP-G2, and LJ-CP8, but the nearby A15 and A17 mutations do not affect binding of these mAbs. Also, the A9, A16, A23, and A29 mutations specifically block binding of one or three mAbs, but not others, indicating that the human-to-mouse mutations do not induce global conformational changes, and their effects remain local.

Ligand-mimetic mAbs Recognize Discontinuous N-terminal Regions of the β_3 Subunit—There are 17-amino acid-residue differences between human and mouse β_3 in the putative I-domain-like region spanning residues 90–328 (Fig. 1*b*). We introduced human-to-mouse mutations into the putative I-domain-like region of human β_3 alone or in-groups. The human-to-mouse β_3 mutants (total 10) were transiently expressed together with wild-type α_{IIb} cDNA on CHO cells. Since CHO cells express endogenous α_v, but do not express β_3, the human β_3 subunit is expressed as human $\alpha_{IIb}\beta_3$ and hamster α_v/human β_3. The ability of $\alpha_{IIb}\beta_3$ or $\alpha_v\beta_3$ to bind to a panel of mAbs (Table I) was tested in flow cytometry. We found that several human-to-mouse mutations affect binding of function-blocking mAbs (Table IV). Binding of mAb 16N7C2 (anti-β_3, RGD+) is completely blocked by the B3 (W129S/N133T) mutation. Binding of 7E3 and A2A9 is completely blocked by the B6 (D179N/T182N/T183A) mutation and partially blocked by the B3 mutation. Binding of AP-2 and LM609 is completely blocked by the B5 (E171Q/L173I/E174K) mutation. In contrast, these mutations only partially blocked the binding of ligand-mimetic mAbs. Binding of OP-G2 and LJ-CP3 is partially blocked by the B6 mutation.

To determine whether the B6 mutation really affects OP-G2 or LJ-CP3 binding, we studied the effects of combined mutations on OP-G2 and LJ-CP3 binding. The combined B3/B6 mutation completely blocked LJ-CP3 binding and almost completely blocked OP-G2 binding. However, the combined B3/B5 or B6/B9 mutation had only a modest effect on OP-G2 and LJ-CP3 binding. These results suggest that the B3 and B6 binding sites are involved in OP-G2 and LJ-CP3 binding, but the nearby B5 and B9 sites (controls) are probably much less involved (Table V). However, binding of several nonligand-mimetic mAbs (*e.g.* 16N7C2) was not affected by the combined mutations tested. We did not find any β_3 mutations that affect the binding of mAbs 2G12, LJ-CP8, and LJ-P9.

Effect of Human-to-mouse Mutation on Activation-dependent PAC-1 and Fibrinogen Binding—We studied the effect of the several mutations that affect binding of ligand-mimetic mAbs on the activation-dependent binding of PAC-1 (Fig. 3). Binding of FITC-labeled PAC-1 was determined as the difference in FITC fluorescence signal (FL-1) in the presence and absence of the activating anti-$\alpha_{IIb}\beta_3$ mAb PT25-2 in the PE-positive (α_{IIb} positive, FL-2) cell population (Fig. 3*a*). PT25-2 activates $\alpha_{IIb}\beta_3$ but does not activate $\alpha_v\beta_3$ (PT25-2 is specific to $\alpha_{IIb}\beta_3$). PAC-1 binding was completely blocked by the A16 mutation and was reduced by the A23 mutation. PAC-1 binding was partly blocked by the B6 mutation but not by the B3, B5, or control B7 mutation. The combined B3/B6 mutations did not further reduce PAC-1 binding. These results suggest that activation-dependent PAC-1 is similar to LJ-CP3 and OP-G2 in that site A16 is critical for binding, and several other sites (sites A23 and B6) are involved in binding.

Binding of soluble fibrinogen to these mutants was studied to determine whether these mutants still bind to ligands. Binding of FITC-labeled fibrinogen was determined as the difference in FITC fluorescence signal in the presence and absence of the activating mAb PT25-2 in the PE-positive (α_{IIb} positive) cell population (Fig. 3*b*). Fibrinogen bound to the A16 and B6 mutants at a level comparable to or higher than that of wild-type and the control B7 mutant. Binding of soluble fibrinogen to the A23 mutant was lower than that of wild-type or the control mutants, but still detectable. These results suggest that the A16, A23, B3, and B6 mutants still maintain the integrity and ligand binding function of $\alpha_{IIb}\beta_3$. Although the fibrinogen binding function appears to vary from mutant to mutant, this may reflect the reported potential species dif-

TABLE II
Specificity of anti-$\alpha_{IIb}\beta_3$ mAbs to human α_{IIb}

Human α_{IIb} with mouse residues 1–443 was transiently expressed in β_3-CHO cells (which homogeneously express human β_3). Cells were stained with primary mAbs and then FITC-labeled goat anti-mouse IgG and analyzed by flow cytometry. Data are expressed as % positive cells. Clonal β_3-CHO cells (which express hamster α_v/human β_3 hybrid) and $\alpha_{IIb}\beta_3$-CHO cells (which express both hamster α_v/human β_3 hybrid and human $\alpha_{IIb}\beta_3$) were used as controls. Parent CHO cells do not express $\alpha_v\beta_3$.

	Parent CHO	β_3-CHO	$\alpha_{IIb}\beta_3$-CHO	Mouse/human α_{IIb}/β_3
Mouse IgG	0.96	2.81	1.5	1.35
PL98DF6	1.28	2	52.66[a]	49.36[a]
mAb 15	1.68	88.75[a]	91.82[a]	91.27[a]
PT25–2	1.71	1.63	59.76[a]	2.26
D57	1.78	2.1	72.73[a]	69.87[a]
2G12	1.64	1.6	65.45[a]	3.35
A2A9	1.85	2.02	61.1[a]	1.64
AP-2	2.33	1.97	63.61[a]	59.44[a]
LJ-CP8	1.67	1.83	56.34[a]	2.08
LJ-P9	1.55	1.92	71.88[a]	1.53
OP-G2	2.24	2.15	55.93[a]	1.01
LJ-CP3	1.83	2.39	38.81[a]	1.21

[a] Positive reactivity.

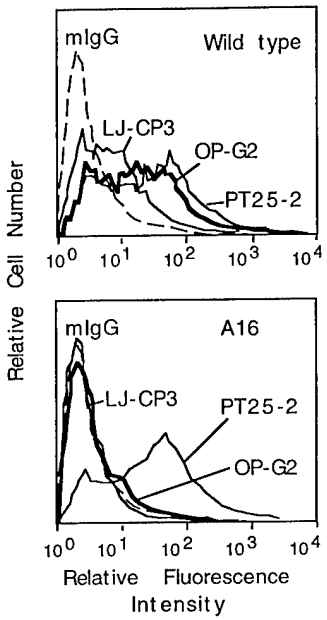

FIG. 2. **Binding of mAbs to wild-type and mutant $\alpha_{IIb}\beta_3$ that are transiently expressed on CHO cells.** Wild-type or mutant α_{IIb} cDNA in pBJ-1 vector was transfected into CHO cells together with wild-type human β_3 cDNA in pBJ-1 vector. After 48 h, cells were harvested and stained first with mAbs LJ-CP3, OP-G2, PT25-2, or control mouse IgG (*mIgG*) and then with FITC-labeled goat anti-mouse IgG. Wt $\alpha_{IIb}\beta_3$ is recognized by all of the anti-$\alpha_{IIb}\beta_3$ mAbs tested. The A16 mutant is recognized by PT25-2 but not by LJ-CP3 or OP-G2.

ference in $\alpha_{IIb}\beta_3$ function (44).

Role of the Predicted Loop (Residues 177–184) of β_3 in Binding to Ligand-mimetic mAbs and Fibrinogen—To determine whether the predicted loop of β_3 (Residues 177–184) that contains site B6 is involved in the binding of ligands and ligand-mimetic mAbs to $\alpha_{IIb}\beta_3$, we swapped this predicted loop of β_3 with the corresponding sequence of β_1. The resulting $\beta_{3\text{-}1\text{-}3}$ mutant cDNA was transfected into CHO cells together with wild-type α_{IIb} cDNA and a neomycin-resistant gene. Cells stably expressing $\alpha_{IIb}\beta_{3\text{-}1\text{-}3}$ were cloned by sorting. Binding of mAbs and fibrinogen was studied by flow cytometry (Table VI). Expression of α_{IIb} was normalized using the anti-α_{IIb} mAb PL98DF6. The results suggest that the $\beta_{3\text{-}1\text{-}3}$ mutation significantly blocks binding of $\alpha_{IIb}\beta_3$ to OP-G2, LJ-CP3, and fibrinogen. The mutation did not affect binding to control mAb 15 (anti-β_3). This suggests that the predicted loop may be critically involved in the binding of $\alpha_{IIb}\beta_3$ to ligand-mimetic mAbs and fibrinogen.

DISCUSSION

What Do the Discontinuous Binding Sites in α_{IIb} for Ligand-mimetic mAbs Tell Us about Structure and Function of α_{IIb}?—The present study provides evidence that two discontinuous sites in α_{IIb} (A16 and A23) are critical for binding to ligand-mimetic mAbs. Several regions/residues that are critical for ligand binding in α_{IIb} have been identified by site-directed mutagenesis or by genetic analysis of natural function-defective $\alpha_{IIb}\beta_3$ mutants (see the Introduction), but whether these regions/residues directly interact with ligands has been unclear. Interestingly, the discontinuous ligand-mimetic mAb binding sites overlap with or are close to several conserved critical residues for ligand binding that have been identified by alanine-scanning mutagenesis (Fig. 4*a*). It should be noted that these conserved critical residues are not changed in human-to-mouse mutations. Site A16 is localized in the predicted loop at the boundary between repeats 2 and 3 of α_{IIb}. We have found that mutating conserved residues Arg-147, Tyr-155, Phe-160, Asp-163, or Arg-165 to Ala blocks binding of fibrinogen and/or ligand-mimetic mAbs (Fig. 4*a*).[1] It has been reported that a patient with Glanzmann's thrombasthenia, who has function-defective α_{IIb}, has a two-amino acid insertion (Arg-Thr) between residues 160 and 161 in this region of the α_{IIb} subunit (45). Mutating Asp-163 in this predicted loop of α_{IIb} to Ala has been shown to block binding of fibrinogen and ligand-mimetic mAbs (45). Site A23 is recognized by the ligand-mimetic mAb LJ-CP3, and is located in the predicted loop at the boundary between repeats 3 and 4 of the α_{IIb} subunit. The nearby D224V mutation of α_{IIb} has recently been shown to block PAC-1 and OP-G2 binding to $\alpha_{IIb}\beta_3$ (46). However, the function of this region has not been identified. We have found that mutating conserved Ser-222, Asp-224, Phe-231, or Asp-232 to Ala blocks binding to fibrinogen and ligand-mimetic mAbs (Fig. 4*a*).[1] The fact that sites A16 and A23 overlap with the α_{IIb} regions that are critical for ligand binding indicates that these residues/regions make direct contact with native ligands. These results are consistent with the proposed β-propeller model of the α subunit (47) in that sites A16 and A23, which are believed to make direct contact with ligands, are spatially close to each other, even though they are separate in the primary structure. In this model, site A9 (an epitope for mAb LJ-P9) is spatially close to sites A16 and A23 (Fig. 5). This is consistent with the function-blocking activity of mAb LJ-P9.

It is possible that site A16 is critically involved in RYD recognition and binding, since site A16 is recognized by all of the RYD-containing ligand-mimetic mAbs, and the A16 mutation completely blocks binding of these mAbs (the effect of the A23 mutation and the human-to-mouse mutations in β_3 on the

TABLE III

Effects of human-to-mouse mutations in α_{IIb} on $\alpha_{IIb}\beta_3$ binding to mAbs

The human-to-mouse α_{IIb} mutants were transiently expressed in CHO cells together with wild-type human β_3. After 48 h, cells were tested for their ability to bind to a panel of anti-$\alpha_{IIb}\beta_3$ mAbs in flow cytometry. Data are expressed as the ratio % positive cells with the mutant $\alpha_{IIb}\beta_3$ to % positive cells with wild type. The data were first normalized for expression, then binding of mAbs relative to wild type was calculated. The % expression of PL98DF6 (a nonfunctional anti-α_{IIb} mAb) was used to normalize the expression of $\alpha_{IIb}\beta_3$ (for LJ-CP3, OP-G2, LJ-CP8, 2G12, PT25–2, LJ-P9, AP2, and A2A9). The % expression of mAb 15 (a nonfunctional anti-β_3 mAb) was used to normalize the expression of β_3 (for D57, 7E3, and 16N7C2). Of the human-to-mouse α_{IIb} mutants tested in this study, only A9, A16, A23, and A29 had a noticeable effect on binding of mAbs tested.

	Wild type	A2	A5	A9	A15	A16	A17	A23	A24	A29
LJ-CP3	1	1.33	0.91	1.02	1.38	0	1.11	0.13	1.02	1.24
OP-G2	1	0.88	0.93	0.84	0.86	0.05	1.02	0.75	0.92	0.89
16N7C2	1	0.98	0.99	0.97	0.99	1.00	0.99	0.98	0.96	0.98
2G12	1	0.72	0.86	0.68	0.72	0.88	1.21	0.94	0.81	0.79
7E3	1	0.98	0.96	0.99	0.99	0.96	0.96	0.96	0.95	0.96
A2A9	1	1.10	1.11	0.96	0.95	0.80	0.80	0.85	0.87	1.10
AP-2	1	1.11	1.05	0.97	0.99	0.92	0.99	1.00	1.04	1.15
LJ-CP8	1	0.83	0.93	0.78	0.81	0	1.11	0.88	0.89	0.88
LJ-P9	1	1.01	0.84	0	0.96	1.17	1.00	1.00	0.80	0.74
PT25–2	1	0.76	0.87	0.74	0.76	1.00	1.06	0.96	0.86	0
D57	1	1.12	0.96	1.04	1.15	1.05	0.85	0.96	1.10	1.15

TABLE IV

Effects of β_3 human-to-mouse mutations on $\alpha_{IIb}\beta_3$ binding to mAbs

The human-to-mouse β_3 mutants were transiently expressed in CHO cells together with wild-type human α_{IIb}. Data are expressed as the ratio % positive cells with the mutant $\alpha_{IIb}\beta_3$ to % positive cells with wild type. Analysis of the reactivity of a panel of mAbs to mutant $\alpha_{IIb}\beta_3$ in flow cytometry and normalization of the results were performed as described in the legend to Table III.

	Wild type	B1	B2	B3	B4	B5	B6	B7	B8	B9	B10
LJ-CP3	1	0.92	0.88	0.90	1.00	0.96	0.25	1.08	0.65	0.89	0.91
OP-G2	1	0.93	0.95	0.79	1.11	0.91	0.57	1.03	0.82	1.18	1.18
16N7C2	1	1.08	1.00	0	1.03	1.00	0.82	0.98	1.06	1.07	1.01
2G12	1	1.04	0.91	1.34	1.10	0.98	1.04	0.93	0.89	1.10	0.92
7E3	1	1.01	1.01	0.58	0.96	1.05	0	1.04	0.91	0.94	1.07
A2A9	1	0.89	1.06	0.69	0.92	0.95	0	0.98	0.87	0.95	1.07
AP-2	1	0.95	1.02	0.92	0.96	0	0.93	1.01	0.95	0.96	1.05
LJ-CP8	1	1.00	0.94	1.16	1.07	0.99	1.08	0.99	0.99	1.13	0.87
LJP9	1	1.06	0.88	1.33	1.13	0.98	1.02	0.96	0.96	1.09	0.91
LM609	1	1.00	0.97	1.03	1.01	0	0.89	0.89	1.13	1.03	1.00
PT25–2	1	1.00	0.90	1.19	1.08	0.98	1.01	0.93	0.94	1.04	0.87
D57	1	0.98	1.03	0.91	0.95	0.20	0.97	1.05	0.95	0.99	1.09

TABLE V

Effects of combined mutations on binding of mAbs to $\alpha_{IIb}\beta_3$

Human-to-mouse β_3 mutants with combined β_3 mutations were transiently expressed in CHO cells together with wild-type human α_{IIb}. Analysis of the reactivity of a panel of mAbs to mutant $\alpha_{IIb}\beta_3$ in flow cytometry and normalization of the results were performed as described in the legend to Table III.

	Wild-type	B3/B5	B3/B6	B6/B9
LJ-CP3	1	0.43	0	0.49
OPG2	1	0.51	0.05	0.53
16N7C2	1	0	0	0.81
2G12	1	1.30	1.34	1.09
7E3	1	0.66	0	0
A2A9	1	0.72	0	0
AP2	1	0	0.78	0.91
LJ-CP8	1	1.36	1.34	1.36
D57	1	0.13	0.96	0.94

binding of ligand-mimetic antibodies is relatively weak and variable compared with that of the A16 mutation and may depend on antibody species.) It is interesting to note that the A16 mutant shows higher fibrinogen binding than wild-type (Fig. 3), although the A16 mutant does not bind to ligand-mimetic antibodies. It is well known that RGD peptide does not effectively block fibrinogen binding to rat and rabbit (44) and mouse $\alpha_{IIb}\beta_3$. It is possible that $\alpha_{IIb}\beta_3$ from these species may have higher affinity to fibrinogen than human $\alpha_{IIb}\beta_3$ due to species difference in site A16. Further biochemical studies of site A16 will be required to address this hypothesis.

The present results indicate that ligand-mimetic mAbs do not recognize the region close to the previously reported putative ligand binding (γ-chain peptide cross-linking) site in repeat 5 of α_{IIb} (2). This suggests that this region is not a major ligand binding site. This idea is consistent with the proposed β-propeller model, since the fibrinogen γ-peptide cross-linking site in repeat 5 of α_{IIb} is located in the lower face of the domain, a predicted nonligand binding site. The regions critical for ligand binding in repeats 2 and 3 (containing sites A16 and A23) are located in the upper face of the model, a predicted ligand binding site (47). It is intriguing that the activating anti-$\alpha_{IIb}\beta_3$ mAb PT25-2 recognizes site A29 in α_{IIb}, which is close to the γ-chain peptide cross-linking site. It is possible that the γ-chain peptide cross-linking site might be an allosteric binding site, which is consistent with the location of this site in the predicted nonligand binding site of the β-propeller model.

What Do the Discontinuous Binding Sites in β_3 for Ligand-mimetic mAbs Tell Us about Structure and Function of β_3?— Although no single human-to-mouse mutation in the β_3 subunit strongly blocks binding of ligand-mimetic mAbs, we provided evidence that the combined B3 and B6 mutation strongly blocks binding of LJ-CP3 and OP-G2 to $\alpha_{IIb}\beta_3$. The fact that more than two mutations are required to block binding of mAbs is not surprising if we assume that these mAbs interact with multiple sites in both subunits for binding. The effect of the combined B3 and B6 mutation is significant, since the nearby control B5 or B9 mutation does not increase the effect of the B3 or B6 mutation. These results indicate that sites B3 and B6 are involved in the binding of these ligand-mimetic mAbs, although the B3 mutation alone has no effect. Site B6 is located in the predicted loop (residues 177–184 of β_3), which has been reported to be critical for ligand binding and specificity (15). Swapping this disulfide-linked predicted loop of β1 with the corresponding β_3 sequence changes the ligand specificity of

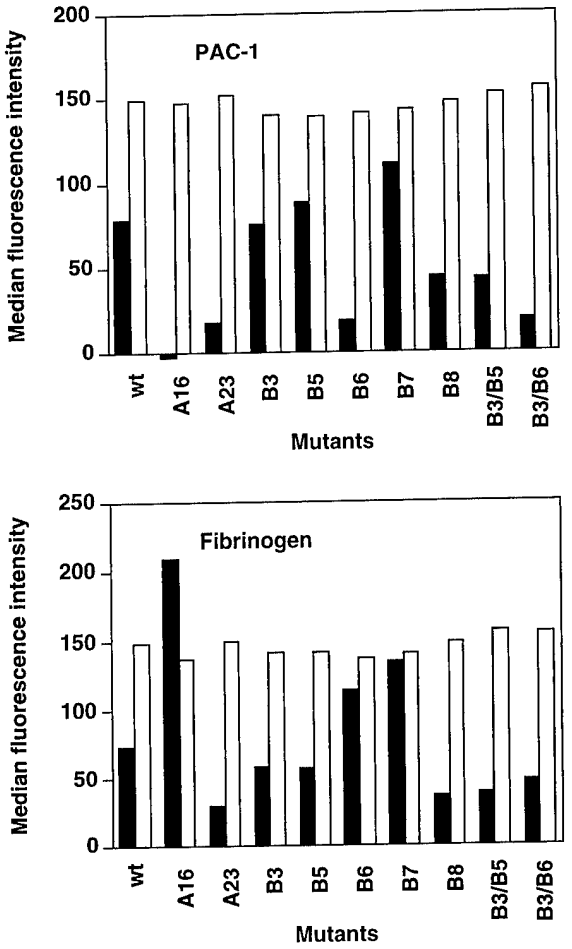

FIG. 3. **Effect of several human-to-mouse mutations in α_{IIb} and β_3 on activation-dependent PAC-1 and fibrinogen binding.** *a*, PAC-1 binding to wild-type and mutant $\alpha_{IIb}\beta_3$. Cells were first incubated with PL98DF6 (anti-human α_{IIb}) followed by PE-conjugated anti-mouse IgG. After washing, cells were incubated with FITC-labeled PAC-1 in the presence of control mouse IgG or PT25-2 (activating anti-$\alpha_{IIb}\beta_3$ mAb) in 5 mM Hepes/Tyrode, 2 mM Ca^{2+}, and 2 mM Mg^{2+} buffer, pH 7.4. Binding of FITC-labeled PAC-1 to the PE-labeled α_{IIb}-positive cell population expressing high level $\alpha_{IIb}\beta_3$ (fluorescence intensity $>10^2$) was examined in FACScan. Data are expressed as a difference in median FITC fluorescent intensity in the presence and absence of PT25-2 (*solid column*). Median PE fluorescence intensity in the cell population used for measurement of PAC-1 binding is shown (*open column*). The data suggest that PAC-1 binding is completely blocked by the A16 mutation and partly blocked by the A23 and B6 mutations. *b*, fibrinogen binding to wild-type and mutant $\alpha_{IIb}\beta_3$. Fibrinogen binding to the cell population expressing high level $\alpha_{IIb}\beta_3$ was determined as described in *a*, except that FITC-fibrinogen was used instead of FITC-PAC-1. Data are expressed as a difference in median FITC fluorescent intensity in the presence and absence of PT25-2 (*solid column*). Median PE fluorescence intensity in the PE-labeled α_{IIb}-positive cell population used for measurement of fibrinogen binding is shown (*open column*). The data suggest that the mutants tested maintain fibrinogen binding, although the A23 mutant shows relatively low fibrinogen binding, and the A16 mutant shows relatively high fibrinogen binding. Parent CHO cells do not show $\alpha_{IIb}\beta_3$-specific fibrinogen binding, since parent CHO cells are PE-negative (FL-2 $<10^2$).

$\alpha_v\beta_3$ (15). Also, fibrinogen C-terminal domains require this predicted loop sequence of β_3 for binding to $\alpha_v\beta_3$ (48). In the present study, we have shown that the $\beta_{3\text{-}1\text{-}3}$ mutant blocks binding of $\alpha_{IIb}\beta_3$ to OP-G2, LJ-CP3, and fibrinogen (Table VI). These results are consistent with the observation that site B6 is involved in the binding of ligand-mimetic mAbs. We found that two function-blocking mAbs, 7E3 and A2A9, also recognize site B6, consistent with their function-blocking activity.

The B3 mutation completely blocks the binding of $\alpha_{IIb}\beta_3$ to

TABLE VI

Effects of the $\beta_{3\text{-}1\text{-}3}$ mutation on $\alpha_{IIb}\beta_3$ binding to ligand-mimetic mAbs and fibrinogen

Cloned cells stably expressing wild type or mutant $\alpha_{IIb}\beta_{3\text{-}1\text{-}3}$ were used. Reactivity to mAbs and binding of FITC-labeled soluble fibrinogen were assayed by flow cytometry. Data are expressed as the ratio of mean fluorescent intensity. The data suggest that the $\beta_{3\text{-}1\text{-}3}$ mutation blocks binding of ligand-mimetic mAbs and fibrinogen to $\alpha_{IIb}\beta_3$.

	Wild type $\alpha_{IIb}\beta_3$	$\alpha_{IIb}/\beta_{3\text{-}1\text{-}3}$	Mutant MFI/wild type MFI ratio
PL98DF6	209 (100)	102 (100)	1
mAb 15	548 (262)	220 (214)	0.82
OP-G2	358 (171)	24.0 (23.3)	0.14
LJ-CP3	134 (64)	3.42 (3.32)	0.052
Fibrinogen	18.7 (8.9)	0.8 (0.78)	0.087

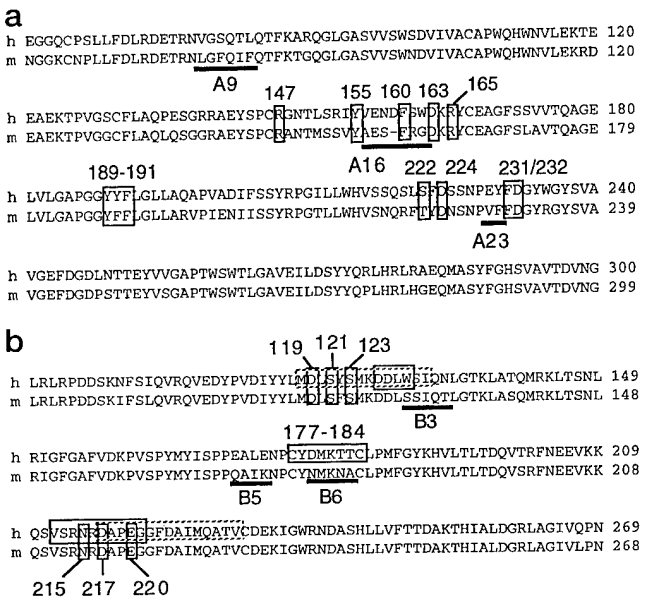

FIG. 4. **Binding sites for function-blocking and/or ligand-mimetic mAbs are close to or overlap with several sequences/residues that are critical for ligand binding and specificity.** *a*, sites A9, A16, and A23 for function-blocking and/or ligand-mimetic mAbs are located at the boundary (the 4-1 loop) between repeats 1 and 2, repeats 2 and 3, and repeats 3 and 4, respectively. Sites A16 and A23 are close to or overlap with conserved residues that are critical for ligand binding (*boxed*, see Introduction for references). *b*, sites B3 and B6 are close to or overlap with the sequences that are critical for ligand binding or specificity (*boxed*, see Introduction for references). These results suggest that the conserved critical sequences/residues for ligand binding and specificity that are close to sites A16, A23, B3, and B6 actually make direct contact with ligands.

the RGD-containing anti-β_3 mAb 16N7C2. It is highly likely that the RGD motif of 16N7C2 is involved in its binding to β_3, since this interaction is blocked by echistatin, an RGD-containing disintegrin (35). Intriguingly, site B3 overlaps with the DDLW sequence (residues 126–129), a putative RGD binding site (Fig. 4). The CWDDGWLC peptide is a functional mimic of the ligand binding sites of RGD-directed integrins (10), and the structurally similar DDLW sequence in the integrin β subunit has been proposed to be a putative RGD binding site. Also, this binding site is part of the MDLSYSMKDDLWSI sequence (residues 118–131), to which the RGD-containing peptide has been reported to make a ternary complex with cations (9). This is consistent with the reports that RGD-containing peptides block binding of these ligand-mimetic mAbs to $\alpha_{IIb}\beta_3$ (25–27). Nearby Asp-119, Ser-121, and Ser-123 are critical for the binding of ligands and ligand-mimetic mAbs (19, 21, 49). Taken together, the present results are consistent with the idea that the DDLW sequence, which overlaps with site B3, makes direct contact

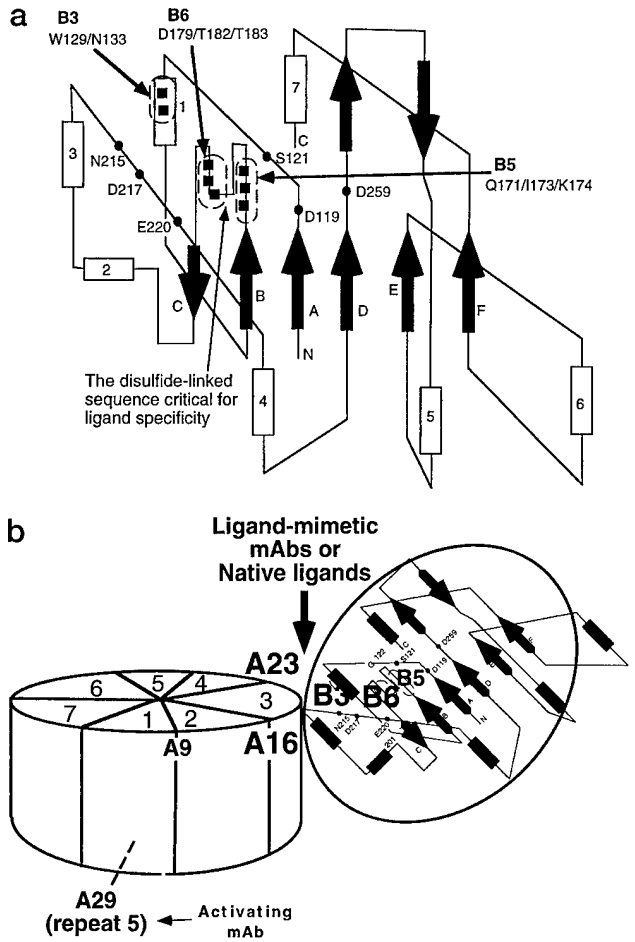

FIG. 5. **Positions of antibody binding sites for function-blocking or ligand-mimetic mAbs in the putative β_3 I-domain (*a*) and the proposed β-propeller domain (*b*).** *a*, the model of the β_3 I-domain was taken from Takagi *et al.* (15) and Tuckwell *et al.* (23) and modified. *Arrows* indicate β-sheets, and *columns* indicate α-helices. *Closed circles* show residues that are critical for ligand binding in β_1 or β_3 (16). In this model, the diverse disulfide-linked sequence that is critical for ligand specificity (residues 177–184 in β_3) (15) is located in the predicted loop, surrounded by conserved oxygenated residues in the upper face of the I-domain-like structure of the β_3 subunit that are critical for ligand binding (*e.g.* Asp-119). The upper face of this domain is predicted to be a ligand binding site, based on its homology to the I-domains of α_M and α_L (23). Site B3 is located in helix 1 and overlaps the putative RGD binding site (10). Site B6 is located in the predicted disulfide-linked sequence that is critical for ligand specificity (15). It should be noted that all of the binding sites for ligand-mimetic or function-blocking mAbs are located on the same side of the model (the putative ligand site) and are predicted to be close to each other. *b*, the approximate positions of the α_{IIb} binding sites are shown. Sites A9, A16, and A23 are located at the boundary between repeats 1 and 2, repeats 2 and 3, and repeats 3 and 4, respectively. Site A29, which is recognized by the activating mAb PT25-2, is located in the lower face (nonligand binding site) of the domain. Also, the potential relative positions of the α_{IIb} proposed β-propeller domain and the putative β_3 I-domain-like structure are shown. In this model, sites A16 and A23 face sites B3 and B6 in the β_3 subunit, generating a ligand binding pocket at the α/β boundary.

with ligands through the RGD motif and is part of the ligand binding site.

It has been reported that $\alpha_{IIb}\beta_3$ may have two distinct ligand binding sites based on kinetic analysis of ligand binding (Refs. 50 and 51 and references therein), but positions of the proposed binding sites are unknown. The RGD-containing mAb 16N7C2 recognizes site B3, which overlaps with the putative RGD binding site in β_3, but this mAb does not require α_{IIb} subunit for binding. The three ligand-mimetic mAbs recognize site A16, which overlaps with critical residues for ligand binding in α_{IIb}. Interestingly, human-to-mouse mutations in β_3 (including B3) have relatively minor effects on binding to ligand-mimetic mAbs compared with the A16 mutation (see above). These results suggest that mAb 16N7C2 and the ligand-mimetic mAbs recognize two separate sites in $\alpha_{IIb}\beta_3$ (B3 and A16, respectively) in an RGD- or RYD-dependent manner. Thus sites A16 and B3 may represent two distinct RGD or RYD recognition and binding sites in $\alpha_{IIb}\beta_3$.

We found that several function-blocking mAbs, including LM609 and AP-2, recognize site B5. These results suggest that site B5 is close to or within the putative ligand binding pocket. Since the noninhibitory mAb D57 recognizes site B5, it is not certain whether site B5 is directly related to ligand binding. Site B5 is located in the large predicted loop protruding from the global structure (Fig. 5). Thus it is possible that antibodies access this loop from different directions or change conformation of the predicted loop in different ways. However, we need more definitive structure of the domain to test these possibilities.

The predicted loop region containing Asn-215, Asp-217, and Glu-220 is critical for the binding of ligand-mimetic mAbs or ligands (21). We did not use human-to-mouse mutagenesis to study whether this region overlaps with the binding sites for ligand-mimetic mAbs, because this region is highly conserved between human and mouse β_3. The present results are useful for evaluating two folding models of the putative I-domain-like structure of the β subunit (21, 23). The present findings (that sites B3, B5, and B6 are located close to each other on the ligand binding side of the β_3 subunit) are consistent with the model by Tuckwell *et al.* (23) (Fig. 5). In this model, the putative RGD binding site (close to site B3) and the predicted loop that is critical for ligand specificity (site B6) are surrounded by conserved oxygenated residues that are critical for binding to ligands and ligand-mimetic mAbs in the β_3 subunit (Asp-119, Ser-121, Ser-123, Asp-217, and Glu-220). Consistently, these conserved residues are critical for binding to OPG2/PAC-1 (19, 21, 49). In the model by Tozer *et al.* (21), site B6 is in the apparently nonligand binding site of the domain, indicating that this model does not fit in with the present mapping results.

Localization of the Binding Sites for Ligand-mimetic mAbs and Ligands at the α/β Boundary—Fig. 5*b* is a model of the $\alpha_{IIb}\beta_3$ globular domain in which the proposed β-propeller domain and the putative I-domain are associated. The regions critical for the binding of ligand-mimetic mAbs and ligands are all in the upper face of both subunits. Interestingly, these results directly demonstrate that the predicted loop at the boundary between repeats 2 and 3 (containing sites A16 and A23) in the proposed β-propeller domain faces the metal ion-dependent adhesive site (MIDAS) region of the putative β_3 I-domain (containing sites B3 and B6) in the quaternary structure (Fig. 5). These results predict that these binding sites for ligand-mimetic mAbs and native ligands constitute a ligand binding pocket at the α/β boundary. The positions of binding sites A9, A16, B3, B5, or B6 in this model are consistent with the function-blocking activity of several nonligand-mimetic mAbs (*e.g.* 7E3, LJ-P9). It is somewhat surprising that the binding of mAbs that are known to be complex-specific can be completely inhibited by substitutions in single subunits. One possibility is that one subunit is involved in antibody specificity by regulating the accessibility to the epitope region.

In summary, we have established that ligand-mimetic antibodies bind to several discontinuous sites in both α_{IIb} and β_3 subunits. It is likely that this unique binding property is related to their ligand-mimetic property (cation and activation dependence). These binding sites are close to or overlapping

with residues/regions that are critical for ligand binding, suggesting that native ligands (*e.g.* fibrinogen) make direct contact with these discontinuous binding sites in both subunits. These results are consistent with the previous assumption that ligand-mimetic mAbs may have structural and functional similarities to native ligands. It would be interesting to study whether the present model of $\alpha_{IIb}\beta_3$ may be applicable to other non-I domain integrins.

Acknowledgments—We thank D. Cheresh, B. S. Coller, H. Deckmyn, M. H. Ginsberg, M. Handa, Y. Ikeda, T. Kunicki, J. C. Loftus, Z. M. Ruggeri, S. J. Shattil, S. Tomiyama, V. Woods, and J. Ylanne for valuable reagents. We also thank S. J. Shattil for critical reading of the manuscript, K. K. Tieu for excellent technical assistance, and A. Ewers for help in preparing the manuscript.

REFERENCES

1. Loftus, J. C., and Liddington, R. C. (1997) *J. Clin. Invest.* **99,** 2302–2306
2. D'Souza, S., Ginsberg, M. H., Burke, T. A., and Plow, E. F. (1990) *J. Biol. Chem.* **265,** 3440–3446
3. D'Souza, S., Ginsberg, M. H., Matsueda, G. R., and Plow, E. F. (1991) *Nature* **350,** 66–68
4. Gulino, D., Boudignon, C., Zhang, L. Y., Concord, E., Rabiet, M. J., and Marguerie, G. (1992) *J. Biol. Chem.* **267,** 1001–1007
5. Kamata, T., Irie, A., and Takada, Y. (1996) *J. Biol. Chem.* **271,** 18610–18615
6. Lee, J.-O., Rieu, P., Arnaout, M. A., and Liddington, R. (1995) *Cell* **80,** 631–638
7. Loftus, J. C., Smith, J. W., and Ginsberg, M. H. (1994) *J. Biol. Chem.* **269,** 25235–25238
8. D'Souza, S., Ginsberg, M. H., Burke, T. A., Lam, S. C.-T., and Plow, E. F. (1988) *Science* **242,** 91–93
9. D'Souza, S. E., Haas, T. A., Piotrowicz, R. S., Byers-Ward, V., McGrath, E., Soule, H. R., Cierniewski, C., Plow, E. F., and Smith, J. W. (1994) *Cell* **79,** 659–667
10. Pasqualini, R., Koivunen, E., and Ruoslahti, E. (1995) *J. Cell Biol.* **130,** 1189–1196
11. Cook, J., Trybulec, M., Lasz, E., Khan, S., and Niewiarowski, S. (1992) *Biochem. Biophys. A.* **1119,** 312–321
12. Lasz, E., McLane, M., Trybulec, M., Kowalska, M., Khan, S., Budzynski, A., and Niewiarowski, S. (1993) *Biochem. Biophys. Res. Commun.* **190,** 118–124
13. Charo, I. F., Nannizzi, L., Phillips, D. R., Hsu, M. A., and Scarborough, R. M. (1991) *J. Biol. Chem.* **266,** 1415–1421
14. Steiner, B., Trzeciak, A., Pfenninger, G., and Kouns, W. (1993) *J. Biol. Chem.* **268,** 6870–6873
15. Takagi, J., Kamata, T., Meredith, J., Puzon-McLaughlin, W., and Takada, Y. (1997) *J. Biol. Chem.* **272,** 19794–19800
16. Puzon-McLaughlin, W., and Takada, Y. (1996) *J. Biol. Chem.* **271,** 20438–20443
17. Takada, Y., Ylanne, J., Mandelman, D., Puzon, W., and Ginsberg, M. (1992) *J. Cell Biol.* **119,** 913–921
18. Kamata, T., Puzon, W., and Takada, Y. (1995) *Biochem. J.* **305,** 945–951
19. Bajt, M. L., and Loftus, J. C. (1994) *J. Biol. Chem.* **269,** 20913–20919
20. Goodman, T. G., and Bajt, M. L. (1996) *J. Biol. Chem.* **271,** 23729–23736
21. Tozer, E. C., Liddington, R. C., Sutcliffe, M. J., Smeeton, A. H., and Loftus, J. C. (1996) *J. Biol. Chem.* **271,** 21978–21984
22. Huang, X., Chen, A., Agrez, M., and Sheppard, D. (1995) *Am. J. Respir. Cell Mol. Biol.* **13,** 245–251
23. Tuckwell, D., and Humphries, M. (1997) *FEBS Lett.* **400,** 297–303
24. Lin, E. C. K., Ratnikov, B. I., Tsai, P. M., Gonzalez, E. R., McDonald, S., Pelletier, A. J., and Smith, J. W. (1997) *J. Biol. Chem.* **272,** 14236–14243
25. Shattil, S. J., Hoxie, J. A., Cunningham, M., and Brass, L. F. (1985) *J. Biol. Chem.* **260,** 11107–11114
26. Tomiyama, Y., Brojer, E., Ruggeri, Z. M., Shattil, S. J., Smiltneck, J., Gorski, J., Kumar, A., Kieber-Emmons, T., and Kunicki, T. J. (1992) *J. Biol. Chem.* **267,** 18085–18092
27. Niiya, K., Hodson, E., Bader, R., Byers-Ward, V., Koziol, J. A., Plow, E. F., and Ruggeri, Z. M. (1987) *Blood* **70,** 475–483
28. Prammer, K. V., Boyer, J., Ugen, K., Shattil, S. J., and Kieber-Emmons, T. (1994) *Receptor* **4,** 93–108
29. Frelinger, A. L., III, Cohen, I., Plow, E. F., Smith, M. A., Roberts, J., Lam, S. C., and Ginsberg, M. H. (1990) *J. Biol. Chem.* **265,** 6346–6352
30. Pidard, D., Montgomery, R. R., Bennett, J. S., and Kunicki, T. J. (1983) *J. Biol. Chem.* **258,** 12582–12586
31. Woods, V. L. J., Oh, E. H., Mason, D., and McMillan, R. (1984) *Blood* **63,** 368–375
32. Ylanne, J., Hormia, M., Jarvinen, M., Vartio, T., and Virtanen, I. (1988) *Blood* **72,** 1478–1486
33. Tomiyama, Y., Tsubakio, T., Piotrowicz, R. S., Kurata, Y., Loftus, J. C., and Kunicki, T. J. (1992) *Blood* **79,** 2303–2312
34. Tokuhira, M., Handa, M., Kamata, T., Oda, A., Katayama, M., Tomiyama, Y., Murata, M., Kawai, Y., Watanabe, K., and Ikeda, Y. (1996) *Thromb. Haemostasis* **76,** 1038–1046
35. Deckmyn, H., Stanssens, P., Hoet, B., Declerck, P. J., Lauwereys, M., Gansemans, Y., Tornai, I., and Vermylen, J. (1994) *Br. J. Haematol.* **87,** 562–571
36. Coller, B. S. (1985) *J. Clin. Invest.* **76,** 101–108
37. Cheresh, D. A., Smith, J. W., Cooper, H. M., and Quaranta, V. (1989) *Cell* **57,** 59–69
38. Deng, W. P., and Nickoloff, J. A. (1992) *Anal. Biochem.* **200,** 81–88
39. Xia, Z., Wong, T., Liu, Q., Kasirer-Friede, A., Brown, E., and Frojmovic, M. M. (1996) *Br. J. Haematol.* **93,** 204–214
40. Goto, S., Salomon, D. R., Ikeda, Y., and Ruggeri, Z. M. (1995) *J. Biol. Chem.* **270,** 23352–23361
41. Rinderknecht, H. (1962) *Nature* **193,** 167–168
42. Hughes, P. E., O'Toole, T. E., Ylanne, J., Shattil, S. J., and Ginsberg, M. H. (1995) *J. Biol. Chem.* **270,** 12411–12417
43. Takada, Y., and Puzon, W. (1993) *J. Biol. Chem.* **268,** 17597–17601
44. Harfenist, E. J., Packham, M. A., and Mustard, J. F. (1988) *Blood* **71,** 132–136
45. Honda, S., Tomiyama, Y., Shiraga, M., Tadokoro, S., Takamatsu, J., Saito, H., Yoshiyuki, K., and Matsuzawa, Y. (1998) *J. Clin. Invest.* **102,** 1183–1192
46. Tozer, E. C., Baker, E. K., Ginsberg, M. H., and Loftus, J. C. (1999) *Blood* **93,** 918–924
47. Springer, T. (1997) *Proc. Natl. Acad. Sci. U. S. A.* **94,** 65–72
48. Yokoyama, K., Zhang, X.-P., Medved, L., and Takada, Y. (1999) *Biochemistry* **38,** 5872–5877
49. Loftus, J. C., O'toole, T. E., Plow, E. F., Glass, A., Frelinger, A. L., and Ginsberg, M. H. (1990) *Science* **249,** 915–918
50. Cierniewski, C. S., Byzova, T., Papierak, M., Haas, T. A., Niewiarowska, J., Zhang, L., Cieslak, M., and Plow, E. F., (1999) *J. Biol. Chem.* **274,** 16923–16932
51. Hu, D. D., White, C. A., Panzer-Knodle, S., Page, J. D., Nicholson, N., and Smith, J. W., (1999) *J. Biol. Chem.* **274,** 4633–4639
52. Bennett, J., Hoxie, J., Leitman, S., Vilaire, G., and Cines, D. (1983) *Proc. Natl. Acad. Sci. U. S. A.* **80,** 2417–2421